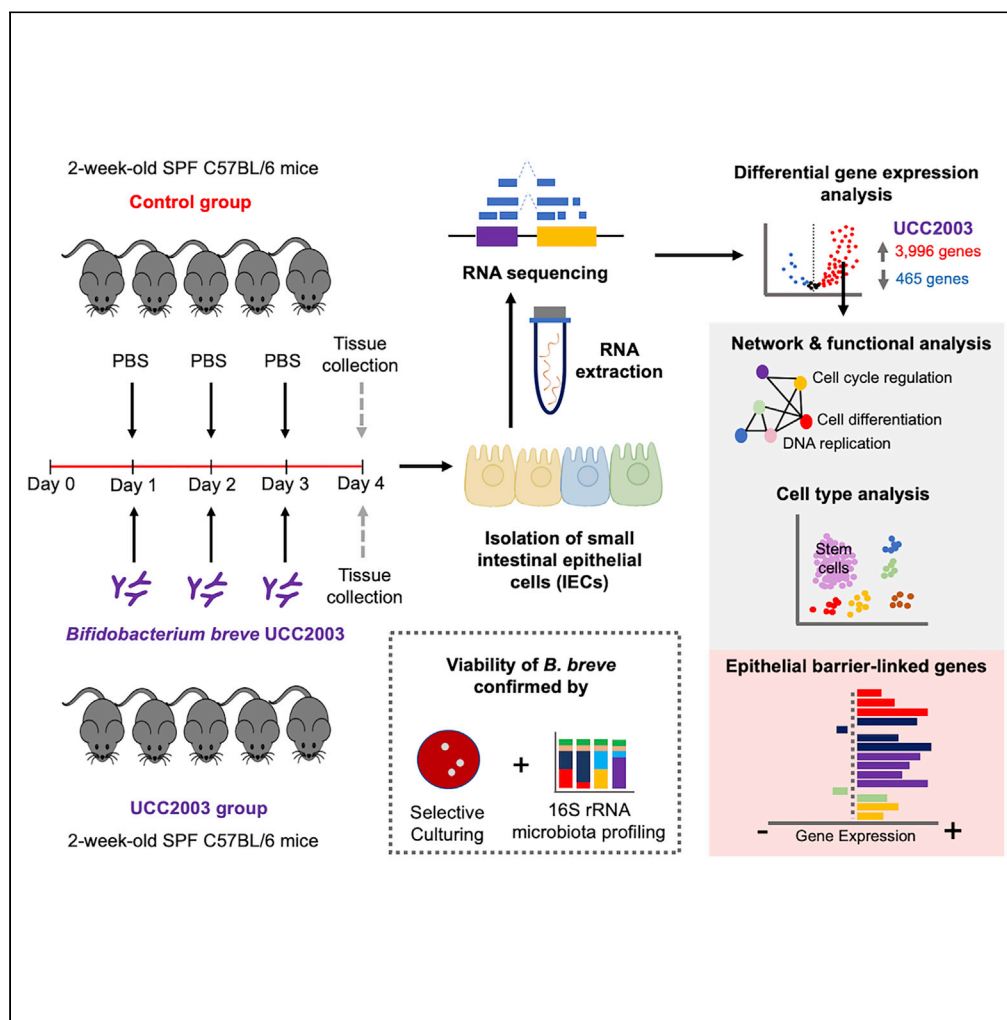


Article

Bifidobacterium breve UCC2003 Induces a Distinct Global Transcriptomic Program in Neonatal Murine Intestinal Epithelial Cells



Raymond Kiu, Agatha Treveil, Lukas C. Harnisch, ..., Douwe van Sinderen, Tamas Korcsmaros, Lindsay J. Hall

lindsay.hall@quadram.ac.uk

HIGHLIGHTS

B. breve administration significantly alters the murine neonatal IEC transcriptome

Genes/pathways involved in epithelial barrier function are particularly impacted

Bifidobacterium may target the IEC stem cell compartment to induce regeneration



Article

Bifidobacterium breve UCC2003 Induces a Distinct Global Transcriptomic Program in Neonatal Murine Intestinal Epithelial Cells

Raymond Kiu,¹ Agatha Treveil,^{1,2} Lukas C. Harnisch,¹ Shabhonam Caim,¹ Charlotte Leclaire,¹ Douwe van Sinderen,³ Tamas Korcsmaros,^{1,2} and Lindsay J. Hall^{1,4,5,6,7,*}**SUMMARY**

The underlying health-driving mechanisms of *Bifidobacterium* during early life are not well understood, particularly how this microbiota member may modulate the intestinal barrier via programming of intestinal epithelial cells (IECs). We investigated the impact of *Bifidobacterium breve* UCC2003 on the transcriptome of neonatal murine IECs. Small IECs from two-week-old neonatal mice administered *B. breve* UCC2003 or PBS (control) were subjected to global RNA sequencing, and differentially expressed genes, pathways, and affected cell types were determined. We observed extensive regulation of the IEC transcriptome with ~4,000 genes significantly up-regulated, including key genes linked with epithelial barrier function. Enrichment of cell differentiation pathways was observed, along with an overrepresentation of stem cell marker genes, indicating an increase in the regenerative potential of the epithelial layer. In conclusion, *B. breve* UCC2003 plays a central role in driving intestinal epithelium homeostatic development during early life and suggests future avenues for next-stage clinical studies.

INTRODUCTION

Bifidobacterium represents a keystone member of the early life gut microbiota (Arrieta et al., 2014; O'Neill et al., 2017; Derrien et al., 2019). Certain species and strains are found at high levels in vaginally delivered breast-fed infants including *Bifidobacterium longum* subsp. *infantis*, *B. longum* subsp. *longum*, *Bifidobacterium bifidum*, *Bifidobacterium pseudocatenulatum*, and *Bifidobacterium breve* (Dominguez-Bello et al., 2010; Mikami et al., 2012; Nagpal et al., 2017; Stewart et al., 2018). As a dominant member of the neonatal gut microbiota, *Bifidobacterium* is associated with metabolism of breast milk, modulation of host immune responses, and protection against infectious diseases (Fukuda et al., 2012; Ling et al., 2016; Robertson et al., 2020; Lawson et al., 2020; Patole et al., 2016; Baucells et al., 2016; Jacobs et al., 2013; Plummer et al., 2018). However, the mechanisms driving improved health outcomes during early life are largely underexplored and are likely strain dependent.

A key interface between *Bifidobacterium* and the host is the intestinal epithelial cell (IEC) barrier (Thoo et al., 2019; Groschwitz and Hogan, 2009). Previous studies have indicated that certain strains of *Bifidobacterium* specifically modulate IEC responses during inflammatory insults, which may help protect from certain gut disorders (Hsieh et al., 2015; Srutkova et al., 2015; Grimm et al., 2015). In murine experimental models, previous work by our group has shown that infant-associated *B. breve* UCC2003 modulates cell death-related signaling molecules, which in turn reduces the number of apoptotic IECs (Hughes et al., 2017). This protection from pathological IEC shedding appeared to be via the *B. breve* exopolysaccharide (EPS) capsule and the host-immune adaptor protein MyD88. Another strain of *B. breve*, NumRes 204 (commercial strain) has also been shown to up-regulate the tight junction (TJ) proteins Claudin 4 and Occludin in a mouse colitis model (Zheng et al., 2014; Plantinga et al., 2011).

Many of the studies to date have focused on the role of *Bifidobacterium* and modulation of IECs in the context of acute or chronic gut inflammation, with expression profiling limited to specific immune or apoptosis signaling targets (Plaza-Diaz et al., 2014; Riedel et al., 2006; Liu et al., 2010; Hsieh et al., 2015). As many of these studies have involved pre-colonization of the gut with *Bifidobacterium* strains, followed

¹Gut Microbes & Health, Quadram Institute Bioscience, Norwich Research Park, Norwich NR4 7UQ, UK

²Earlham Institute, Norwich Research Park, Norwich NR4 7UZ, UK

³APC Microbiome Ireland & School of Microbiology, University College Cork, Cork T12YT20, Ireland

⁴Norwich Medical School, University of East Anglia, Norwich Research Park, Norwich NR4 7TJ, UK

⁵Chair of Intestinal Microbiome, School of Life Sciences, Technical University of Munich, 85354 Freising, Germany

⁶ZIEL – Institute for Food & Health, Technical University of Munich, 85354 Freising, Germany

⁷Lead Contact

*Correspondence: lindsay.hall@quadram.ac.uk
<https://doi.org/10.1016/j.isci.2020.101336>



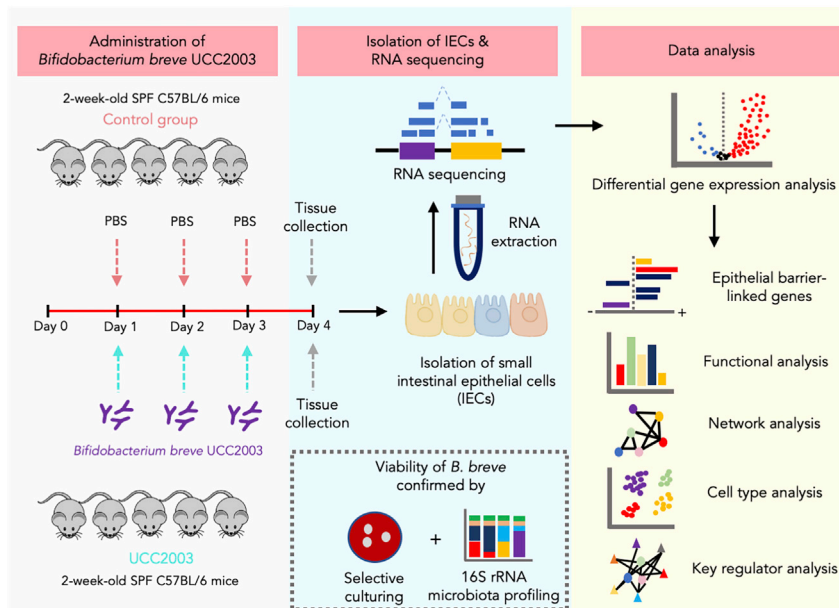


Figure 1. Schematic Representation of the Study Design and *In Silico* Analysis Workflow

by inflammatory insult, this suggests that initial priming during normal “healthy” conditions may modulate subsequent protective responses. Furthermore, these studies have often been performed in adult mice rather than exploring effects during the early life developmental window, where *Bifidobacterium* effects are expected to be most pronounced. Previous work has indicated that there is significant modulation of the neonatal IEC transcriptome in response to gut microbiota colonization, but to date no studies have probed how particular early life-associated microbiota members, like *Bifidobacterium*, may modulate neonatal IEC responses (Pan et al., 2018). Thus, to understand if and how *Bifidobacterium* may modulate IEC homeostasis during the early life developmental window, we administered *B. breve* UCC2003 to neonatal mice and profiled transcriptional responses in isolated small intestine IECs using global RNA sequencing (RNA-seq). Our analysis indicated whole-scale changes in the transcriptional program of IECs (~4,000 significantly up-regulated genes) that appear to be linked to cell differentiation/proliferation and immune development. Notably the stem cell compartment of IECs seemed to elicit the strongest gene signature. These data highlight the role of *B. breve* UCC2003 in driving early life epithelial cell differentiation and maturation, impacting intestinal integrity and immune functions, which provides a mechanistic basis for understanding associated health-promoting effects.

RESULTS

To examine the effects of *B. breve* UCC2003 on the transcriptional profiles of host IECs under homeostatic conditions, we extracted RNA from isolated IECs of healthy 2-week-old neonatal mice (control group) and mice gavaged with *B. breve* UCC2003 for three consecutive days ($n = 5$ per group). Isolated RNAs from IECs were subjected to RNA-seq to determine global mRNA expression (Figure 1). Subsequently, Differential Gene Expression analysis was performed to understand *B. breve*-associated gene regulation.

Minimal Impact of *B. breve* UCC2003 on the Wider Neonatal Gut Microbiota

Initially, we examined for the presence of *B. breve* UCC2003 in the gut microbiome and impact on the wider microbiota using culture and 16S rRNA microbiota profiling approaches (Figures 2A and 2B). We observed high levels of *B. breve* UCC2003 across the 4 days in fecal samples, with higher levels of viable *B. breve* UCC2003 within the colon ($\sim 10^8$ CFU/g [colony-forming unit]), when compared with the small intestine ($\sim 10^5$ CFU/g; Figure 2B). Based on 16S rRNA analysis, relative abundance of *Bifidobacterium* increased significantly in the UCC2003 group ($p = 0.012$) following bacterial administration, whereas the control group displayed very low relative *Bifidobacterium* abundance ($\sim 0.01\%$; Figure 2C). Principal-component analysis (PCA) on gut microbiota profiles (control versus UCC2003) showed a distinct change in microbial

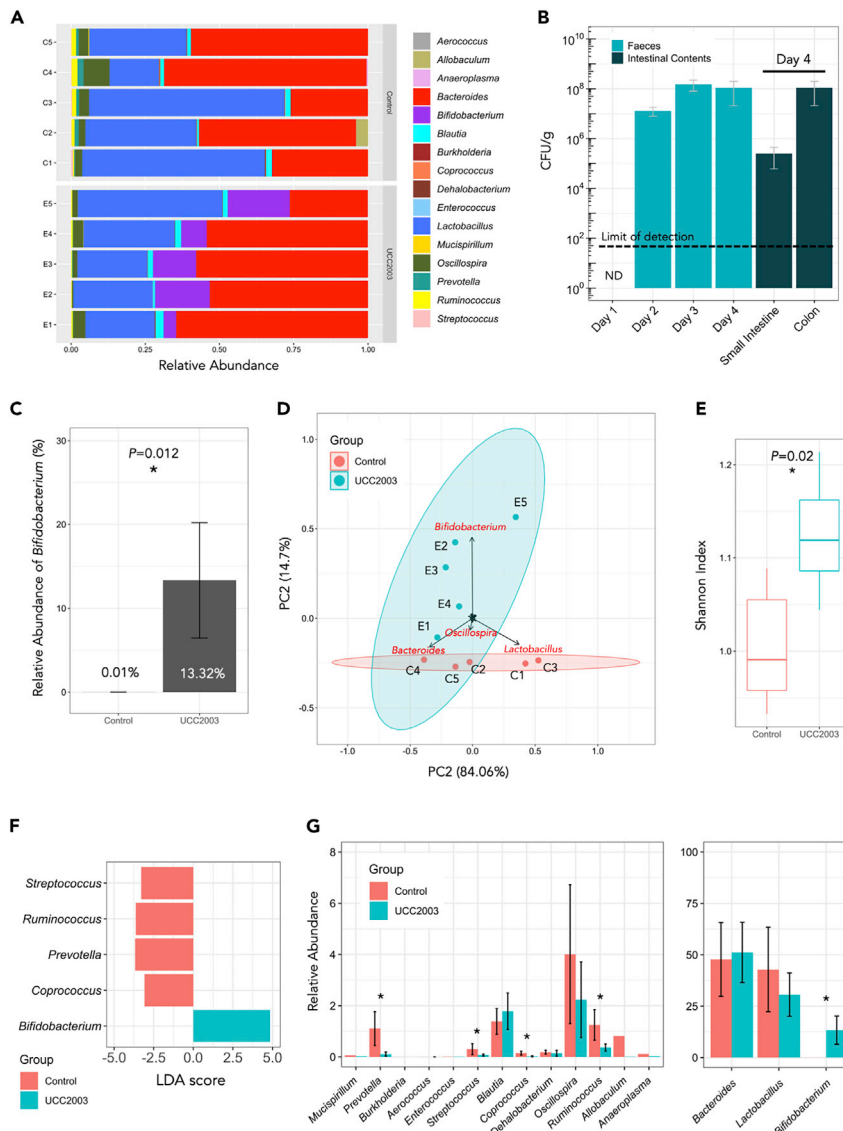


Figure 2. 16S rRNA Amplicon Sequencing Analysis of Murine Intestinal Microbiota

- (A) Genus-level 16S rRNA gene profiling of mice gut microbiota on day 4 (control versus UCC2003).
 (B) Dynamics of *B. breve* UCC2003 load (CFU/g) from day 1 (before *B. breve* administration) through day 4. *B. breve* was present in intestines throughout (small intestines and colon; on day 4). ND, non-detectable. Data are represented as mean \pm SD.
 (C) Relative abundance of genus *Bifidobacterium* in UCC2003 group is significantly increased.
 (D) Principal-component analysis on mice gut microbiota (control versus UCC2003 based on genus-level metatransomics).
 (E) Shannon diversity index on mice gut microbiota (control versus UCC2003). Data are represented as mean \pm SD. Significance test: t test (* $p < 0.05$; two-sided).
 (F) Linear Discriminant Analysis (LDA) showing enriched taxa in each group (control versus UCC2003).
 (G) Relative abundance comparison of all genera. * $p < 0.05$ (LDA).

community composition in the UCC2003 group primarily driven by increased relative abundance of *Bifidobacterium*, which may also correlate with increased overall microbial diversity in the UCC2003 group (Figures 2D and 2E). Linear Discriminant Analysis also indicated that *Bifidobacterium* was uniquely enriched in UCC2003 group, and that microbiota members with low relative abundance (<2%) such as *Streptococcus*, *Ruminococcus*, *Prevotella*, and *Coprococcus* were significantly lower (Figures 2F and 2G). Overall, administration of *B. breve* UCC2003 appeared to minimally impact the wider gut microbiota, without significantly

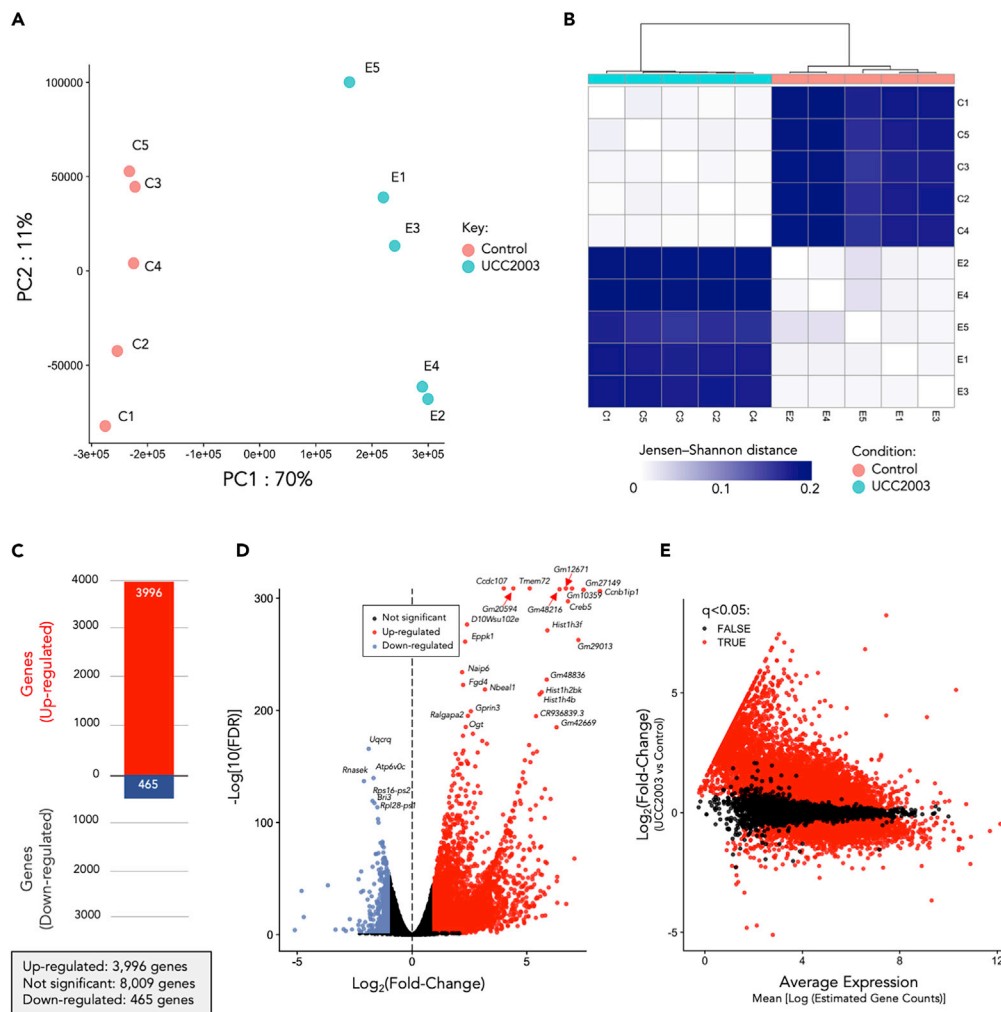


Figure 3. RNA-Seq Analysis and Statistics

- (A) Principal-component analysis showing distinct overall gene expression profiles across all individual samples based on 12,965 highly expressed genes. See also [Table S1](#).
 (B) Clustering of individual RNA-seq samples based on Jensen-Shannon distance. Distinct gene expression profiles were demonstrated between these two groups of samples (control versus UCC2003).
 (C) Total number of differentially expressed genes (DEGs) in UCC2003 group.
 (D) Volcano plot of global gene expression. Up-regulated DEGs are labeled as red dots, whereas down-regulated DEGs are labeled in blue.
 (E) MA plot of global gene expression (plot of log-intensity ratios [M-values] versus log-intensity averages [A-values]).

altering relative abundance of other major resident taxa including *Lactobacillus*, *Bacteroides*, and *Blautia* compared with the control group.

Impact of *B. breve* UCC2003 on the Neonatal Intestinal Epithelial Transcriptome

To understand the distribution of samples based on IEC gene expression profiles we performed PCA analysis ([Figure 3A](#); [Table S1](#)). All samples clustered according to group (control versus UCC2003), suggesting a significant impact of *B. breve* UCC2003 on gene expression profiles, with distance-wise clustering (Jensen-Shannon) also supporting separation of experimental groups ([Figure 3B](#)). To define differentially expressed genes (DEGs), we employed a filter of absolute \log_2 fold change (LFC) > 1.0 (with adjusted $p < 0.05$), which equates to a minimum 2-fold change in gene expression ([Figures 3C–3E](#); [Table S2](#)). After analysis, a total of 3,996 DEGs were significantly up-regulated, whereas 465 genes were significantly down-regulated in *B. breve* UCC2003-supplemented animals when compared with controls ([Figures 3C and 4A](#)). Notably,

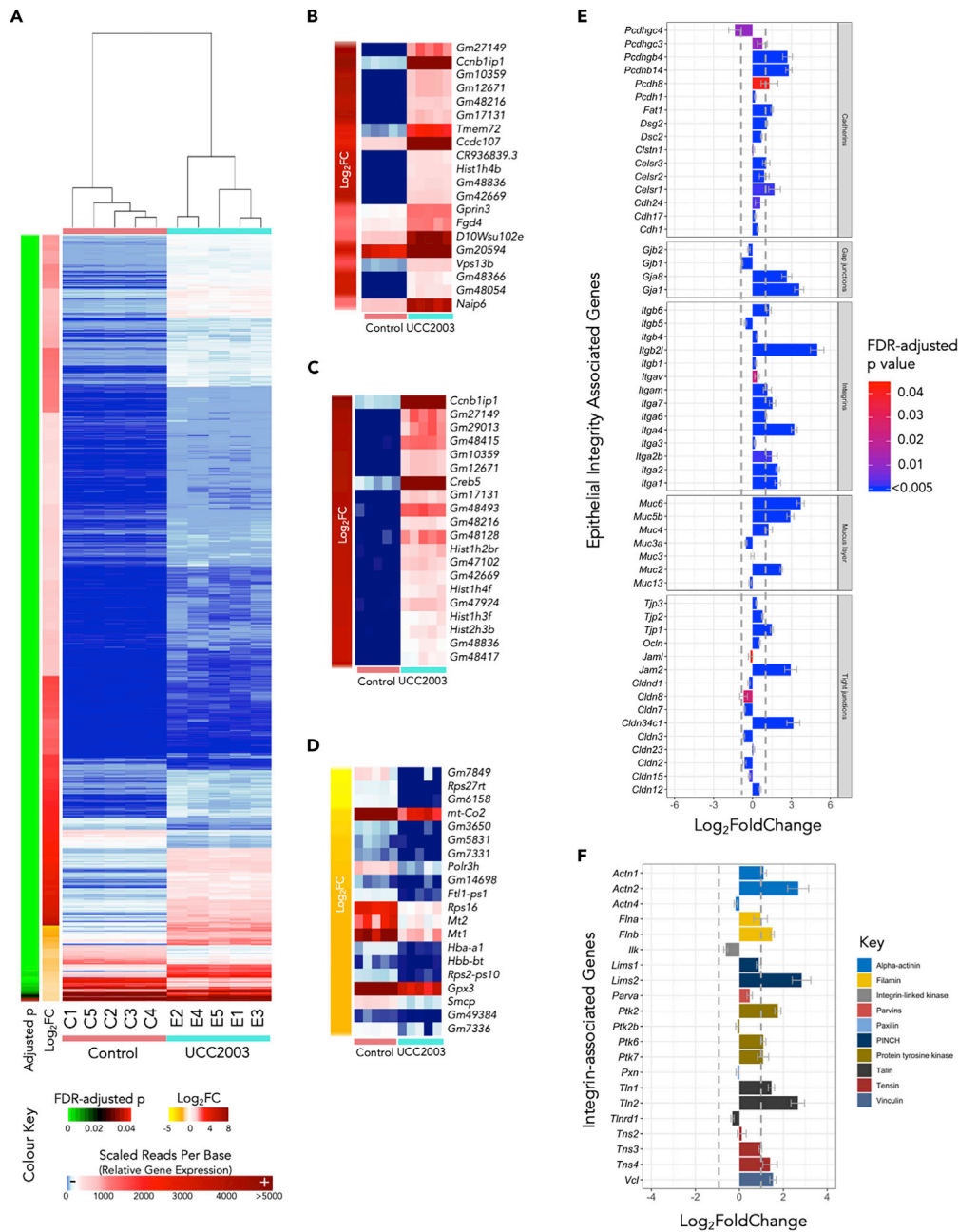


Figure 4. Gene Expression Analysis

(A) Heatmap comparison of gene expression profiles of 4,461 DEGs (control versus UCC2003). See also [Table S2](#).
 (B) Top 20 DEGs ranked by false discovery rate -adjusted p values (q values).
 (C) Top 20 up-regulated DEGs ranked by log₂FC (fold change) values.
 (D) Top 20 down-regulated DEGs ranked by log₂FC values.
 (E) Expression of epithelial integrity associated genes in UCC2003 group (q < 0.05).
 (F) Expression of integrin-associated genes in UCC2003 group. Gray dotted lines in the bar charts indicate the threshold of absolute log₂FC > 1.0. Data are represented as mean ± SE.

we also performed the same experimental protocol on healthy mice aged 10–12 weeks and did not observe any significant DEGs, suggesting that *B. breve* UCC2003 modulation of IECs is strongest within the early life window under homeostatic conditions.

To determine the functional role of DEGs, we examined the most significantly regulated genes ranked by false discovery rate-adjusted p values (or, q values). We first looked at the top 20 up-regulated DEGs in the *B. breve* UCC2003 experimental group (Figure 4B). Most genes annotated with known biological processes had cell differentiation and cell component organization functions including *Ccnb1ip1*, *Hist1h4b*, *Vps13b*, and *Fgd4* (annotated in the PANTHER Gene Ontology [GO] Slim resource). Two genes were involved in cell death and immune system processes, namely, *Naip6* and *Gm20594* (Table S3). When we ranked the top-regulated genes using LFC, we observed increased expression of *Creb5*, which is involved in the regulation of neuropeptide transcription (cAMP response element-binding protein; CREB) (Figure 4C). CREB is also known to regulate circadian rhythm, and we also identified additional circadian-clock-related genes that were significantly up-regulated including *Per2* and *Per3*. We noted that several top down-regulated DEGs were annotated as genes involved in metal binding, or metal-related genes including *Mt1*, *Mt2*, *Hba-a1*, *Hbb-bt*, and *Ftl1-ps1* (Figure 4D; Table S4).

Regulation of Intestinal Epithelial Barrier-Associated Genes

As *B. breve* strains have been previously shown to modulate certain TJ/barrier-related proteins, we next investigated DEGs associated with intestinal epithelial barrier development/intestinal structural organization (Figure 4E). Several TJ structural-associated DEGs were observed, including Claudin-encoding gene *Cldn34c1* (LFC 3.14), Junction Adhesion Molecules-encoding genes *Jam2* (LFC 2.9), and TJ protein (also called Zonula Occludens protein; ZO)-encoding gene *Tjp1* (LFC 1.49). Genes that encode integrins (involved in regulation of intracellular cytoskeleton) also exhibited a trend of increased expression (13/14; 92.8%). Both Piezo genes, which assist in TJ organization, *Piezo1* (LFC 1.25) and *Piezo2* (LFC 1.9), were significantly up-regulated in the *B. breve* UCC2003-treated group.

Over 90% cadherins, proteins associated with the assembly of adherens junctions (Figure 4E), were up-regulated, including *Pcdhb14* (LFC 2.8), *Pcdhgb4* (LFC 2.7), *Pcdh8* (LFC 1.3), *Fat1* (LFC 1.5), and *Dsg2* (LFC 1.1). Interestingly, several genes (4/7; 57.1%) involved in mucous layer generation were significantly up-regulated in the UCC2003 experimental group, including *Muc2* (LFC 2.2), *Muc6* (LFC 3.7), *Muc5b* (LFC 2.9), and *Muc4* (LFC 1.24). Genes *Gja1* (LFC 3.59) and *Gjb8* (LFC 2.63) that encode gap junction proteins were also up-regulated. In addition, we also investigated the differential expression of genes associated with integrin assembly and downstream integrin signaling pathways (Figure 4F). Over 70% (16/21) of these genes were up-regulated, with 52.3% (11/21) significantly increased in gene expression in the UCC2003 group (LFC >1.0).

We observed increased expression of genes associated with IEC barrier development including cadherins, gap junctions, integrins, mucous layer-associated genes, and several key TJ proteins. These strongly induced gene expression profiles suggest that *B. breve* UCC2003 is involved in enhancing epithelial barrier development in neonates.

Modulation of Cell Maturation Processes

We next sought to understand the biological functions of up-regulated DEGs by employing PANTHER GO-Slim functional assignment and process/pathway enrichment analysis (see Figure S1; Tables S5 and S6). DEGs were predominantly involved in general biological processes including cellular process (901 genes) and metabolic process (597 genes; Table S7). At the molecular function level, DEGs were primarily assigned to binding (868 genes) and catalytic activity (671 genes; Table S8), with Olfactory Signaling Pathway and Cell Cycle (biological) pathways also found to be enriched (Table S9).

To delve further into the data, we constructed a signaling network based on up-regulated DEGs ($n = 3,996$) with the aim of identifying specific gene networks involved in important signaling pathways (Figure 5A). Overall, 1,491 DEGs were successfully mapped (37.3%) to a signaling network that comprised 8,180 genes. Four individual clusters of genes were detected, with functional assignment and pathway analysis implemented on these clusters (Figure 5A). All gene clusters were associated with cell differentiation and maturation, with cluster 1 (68 genes) linked specifically with DNA replication and transcription, cluster 2 (26 genes) with cell growth and immunity, cluster 3 (11 genes) with cell replication, and cluster 4 (72 genes) related to cell cycle and cell division (Table S10).

Intestinal Cell Type Analysis on DEGs Identifies Significant Enrichment of Epithelial Stem Cells

IECs include several absorptive and secretory cell types, namely, enterocytes, Paneth cells, goblet cells, enteroendocrine cells, tuft cells, and stem cells. As these cells perform different functions in the gut, it was

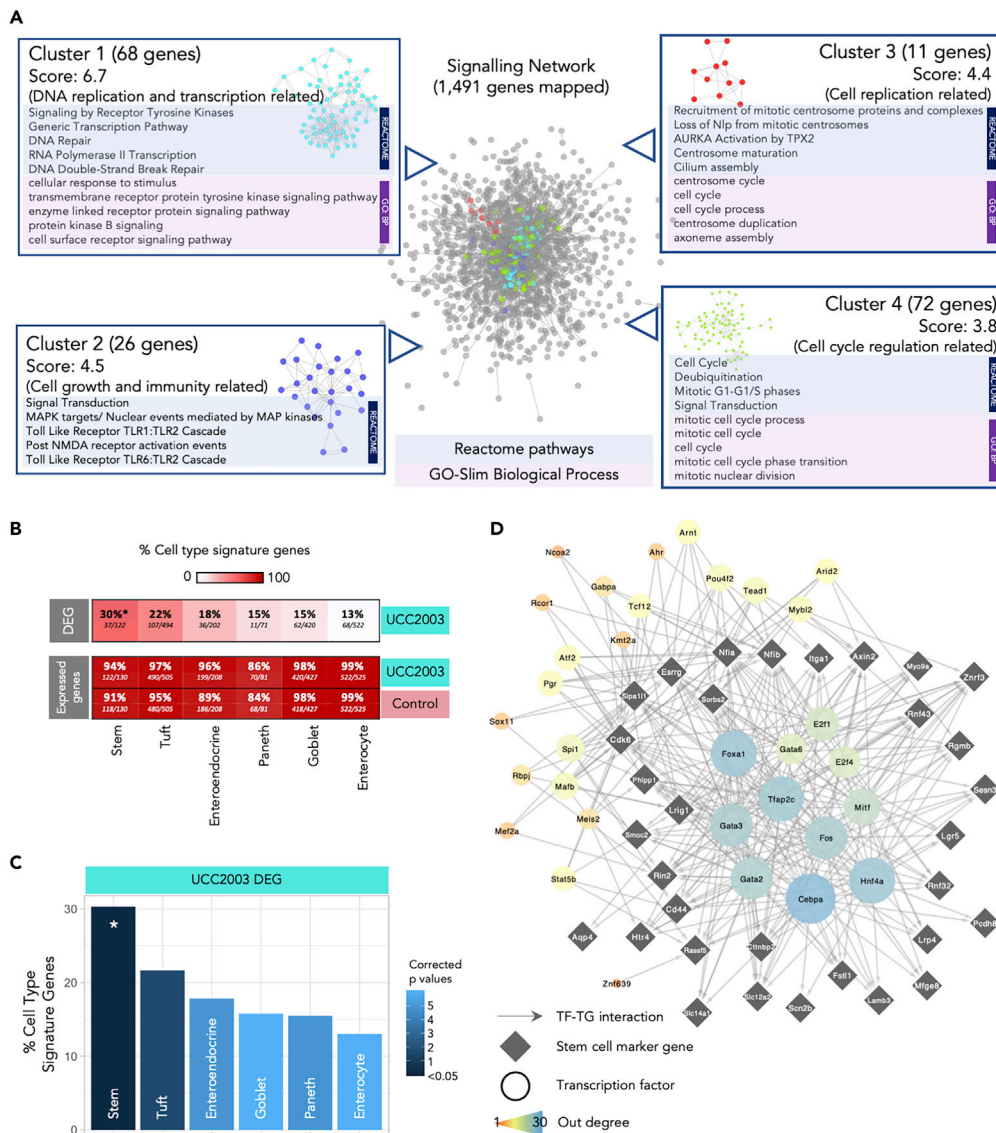


Figure 5. Signaling Network Analysis, IEC Subtyping, and Key Regulator Analysis

(A) Cluster analysis of signaling network for significantly up-regulated genes ($n = 3,996$). Representative enriched pathways (Reactome) and GO terms (Biological Process) identified in each individual cluster were listed alongside. See also [Table S10](#).

(B) Heat plot showing percentage of cell type signature genes in DEG and expressed genes (both control and UCC2003 groups). All expressed genes are well represented in IEC cell type signature genes.

(C) Cell type analysis on IEC DEGs using known cell-specific signature genes. Stem cells were statistically over-represented in DEGs. $*p < 0.05$. See also [Table S11](#).

(D) Key regulators of stem cell DEGs.

important to understand whether *B. breve* UCC2003 had a cell type-specific effect on the intestinal epithelium. Using known cell type-specific gene markers ([Haber et al., 2017](#)), we identified cell type gene signatures modulated within the UCC2003 group ([Figures 5B and 5C](#)). Importantly, all cell type markers were well represented in the expressed genes of the whole IEC transcriptomics data from both groups (control + UCC2003), thus validating the presence of all IEC types in our study data ([Figure 5B](#)). Cell type analysis of genes differentially expressed after *B. breve* UCC2003 supplementation revealed that stem cell marker genes were significantly enriched (30%; $p < 0.05$) among the six IEC types ([Table S11](#)). Signatures of other cell types were also present (linking to marker genes in the DEG list) but not significantly overrepresented:

tuft cells (22%), enteroendocrine cells (18%), goblet cells (15%), Paneth cells (15%), and enterocytes (13%; Figure 5C). These data indicated that intestinal epithelial stem cells, cells primarily involved in cell differentiation, were the primary cell type whose numbers and transcriptomic program were regulated by *B. breve* UCC2003.

Further investigation of this stem cell signature revealed that of the 37 differentially expressed marker genes, 35 are up-regulated in the presence of *B. breve* UCC2003. This indicates an increase in the quantity of stem cells or semi-differentiated cells in the epithelium, consistent with the overrepresentation of cell cycle- and DNA replication-associated genes observed in the whole differential expression dataset. Functional analysis of the 37 stem cell signature genes revealed only one overrepresented process—Regulation of Frizzled by ubiquitination ($p < 0.05$), which is a subprocess of WNT signaling. WNT signaling is important in maintaining the undifferentiated state of stem cells (Nusse, 2008).

Finally, we employed a network approach to predict key transcription factor (TF) regulators of the differentially expressed stem cell marker genes, through which *B. breve* UCC2003 may be acting (Figure 5D). Using the TF-target gene database, DoRothEA, we identified expressed TFs known to regulate these genes (Garcia-Alonso et al., 2019; Holland et al., 2019). Five genes had no known and expressed regulator, and thus were excluded. Hypergeometric significance testing was used to identify which of these TFs are the most influential (see Methods for details). This analysis identified 32 TF regulators (Figure 5D). Of these regulators, 12 were differentially expressed in the IEC dataset (all up-regulated): *Fos*, *Gabpa*, *Rcor1*, *Arid2*, *Tead1*, *Mybl2*, *Mef2a*, *Ahr*, *Pgr*, *Kmt2a*, *Ncoa2*, and *Tcf12*. Functional analysis of all the TF regulators and their targeted genes together, revealed overrepresented functions relating to WNT signaling, histone methylation for self-renewal and proliferation of hematopoietic stem cells, and nuclear receptor (incl. estrogen) signaling (Table S12). These data indicate that *B. breve* UCC2003 directly affects key transcriptomic programs that regulate specific signaling processes, particularly within stem cells.

DISCUSSION

The early life developmental window represents a crucial time for microbe-host interactions that impacts health both in the short and longer term. Understanding how specific microbiota members modulate host responses in pre-clinical models may help the design and development of next-stage targeted microbiota therapies in humans. Here we investigated how *B. breve* UCC2003 induces genome-wide transcriptomic changes in small intestine IECs of neonatal mice. We observed that *B. breve* had a global impact on the IEC transcriptome, evidenced by the large number of significantly up-regulated genes and pathways related to cell differentiation and cell proliferation, including genes associated with epithelial barrier function. We propose that *B. breve* may act as a key early life microbiota member driving fundamental cellular responses in murine IECs, particularly within the stem cell compartment, and thus drives epithelial barrier development and maintenance during neonatal life stages. However, further clinical studies would be required to determine if our findings extrapolate to the human setting.

B. breve is known to confer beneficial effect on gut health; however, our knowledge related to the mechanisms underlying these responses is limited. Most studies have focused on targeted immune cells or pathways (during disease and/or inflammation), and to our knowledge no studies have probed global transcriptomic changes within IECs, the frontline physical barrier between bacteria and host (Turroni et al., 2014; Gann, 2010). Our presented findings in a pre-clinical model, namely, ~4,000 up-regulated DEGs and ~450 down-regulated DEGs within the *B. breve* group, indicate that this *Bifidobacterium* strain modulates whole-scale changes within this critical single-cell layer. Notably, we also examined how *B. breve* modulates adult IEC responses; however, we did not observe any significantly differentially regulated genes when compared with control animals. The striking differences in DEGs between these two life points indicate that *B. breve* modulation of IECs is limited to the neonatal window. Dominance of *Bifidobacterium* in early life (including strains of *B. breve*) overlaps with the development and maturation of many host responses, including epithelial barrier integrity. Therefore, presence of these strains would be expected to play an over-sized role in this initial homeostatic priming, which may afford protection against inflammatory insults in later life, as has been shown previously in a mouse model of pathological epithelial cell shedding (Hughes et al., 2017). Further clinical studies would be required to probe these findings in detail to determine their importance during healthy infant development.

Exploring the murine transcriptional responses in more detail revealed that expressions of key genes associated with formation of epithelial barrier components were up-regulated, including major cell junction

protein-encoding genes (75%; 42/56 genes). More specifically, several integrin-associated genes were up-regulated in the presence of UCC2003. Integrins facilitate cell-cell and cell-extracellular matrix adhesion and binding and assembly of the fibronectin matrix that is pivotal for cell migration and cell differentiation (Harburger and Calderwood, 2009; Qin et al., 2004; Mosher et al., 1991). Integrins also play an important role in downstream intracellular signaling that controls cell differentiation, proliferation, and cell survival, including the Raf-MEK-ERK signaling pathway (we also observed enrichment of genes involved in this pathway) (Chernyavsky et al., 2005; Li et al., 2016). Another key intestinal barrier component is represented by TJs, linking complexes between intercellular spaces, and comprise transmembrane proteins including occludins, claudins, zona occludens, and junctional adhesion molecules (Edelblum and Turner, 2009; Groschwitz and Hogan, 2009). Dysfunctional TJ may lead to a “leaky” gut, which is characteristic of numerous intestinal disorders including inflammatory bowel diseases (Krug et al., 2014). Notably, previous work has suggested early life microbiota disruptions (via antibiotic usage) and reductions in *Bifidobacterium* are correlated with increased risk and/or symptoms of ulcerative colitis and Crohn’s disease (Kronman et al., 2012; Hildebrand et al., 2008; Favier et al., 1997; Shaw et al., 2010; Ng et al., 2011). Several clinical studies have indicated that supplementation with certain *Bifidobacterium* strains positively modulate gastrointestinal symptoms of patients, which is corrected with reductions of inflammatory markers in colonic IEC-containing biopsies; however, *B. breve* UCC2003 has not been used clinically in this patient setting (Furrie et al., 2005; Steed et al., 2010). Similar findings have also been reported in different animal models of intestinal inflammation (Philippe et al., 2011; Grimm et al., 2015; Zuo et al., 2014). A wide range of TJ-related genes were up-regulated after UCC2003 supplementation, particularly *Tjp1* (that encodes ZO-1), *Jam2*, and *Claudin34c1*, with a previous study indicating that other *Bifidobacterium* species (i.e., *B. bifidum*) also modulate TJ expression via ZO-1 (Din et al., 2020). These data indicated that specific strains of *Bifidobacterium* may modulate key barrier integrity systems during the neonatal period, and therefore absence of this key initial bacterial-host cross talk may correlate with increased risk of chronic intestinal disorders in later life (Shaw et al., 2010). Intestinal mucus, encoded by *Muc* genes (up-regulated due to *B. breve* UCC2003 in this study), plays a crucial role in colonic protection via formation of a physical barrier between the gut lumen and IECs, and deficiencies in MUC-2 have been linked with experimental colitis and increased inflammation in patients with inflammatory bowel disease (Shirazi et al., 2000; Van der Sluis et al., 2006). We have also observed that *B. breve* UCC2003 significantly increases goblet cell numbers and mucus production (in gnotobiotic and SPF mice; data not shown). Although the mucus layer may impact direct *Bifidobacterium*-IEC interactions, previous studies have indicated that *B. breve* UCC2003 surface molecules, such as EPS and the Tad pilus, may modulate IEC function via signaling through Toll-like receptors (TLRs) (O’Connell Motherway et al., 2019; Hughes et al., 2017). Moreover, bifidobacterial metabolites, such as short-chain fatty acids may also act to modulate the IEC transcriptome, with previous studies indicating enhanced expression of TJs and cadherins via acetate (Hsieh et al., 2015; Ling et al., 2016; Ewaschuk et al., 2008; Lewis et al., 2017).

Further network and functional analysis indicated that clusters of up-regulated DEGs were associated with cell maturation and cell differentiation (as confirmed by cell type-specific analysis), suggesting that neonatal *B. breve* exposure positively modulates IEC cell differentiation, growth, and maturation. Somewhat surprisingly, we did not observe the same type of striking responses in immune pathways, which may be masked by the sheer number of DEGs involved in cellular differentiation and processes. However, pathways such as TLR1 and TLR2 pathways do appear to be enriched (cluster 2 of signaling network analysis). This may link to previous work indicating that the UCC2003 EPS signals via TLR2 to induce MyD88 signaling cascades to protect IECs during intestinal inflammation (Hughes et al., 2017). *B. breve* M-16V was also shown to interact with TLR2 to up-regulate ubiquitin-editing enzyme A20 expression that correlated with increased tolerance to a TLR4 cascade in porcine IECs, further supporting the involvement of *B. breve* in programming key host immunoregulation receptors (Tomosada et al., 2013).

Cell type-specific analysis of DEGs revealed stem cells as the IEC type most affected by *B. breve*, with absorptive enterocytes least affected despite being most accessible to bacteria in the gut. It could be hypothesized that *B. breve* or their secreted metabolites may reach the crypts of the small intestinal epithelium. This has been previously suggested by *in situ* hybridization histology *in vivo* and by *Bifidobacterium*-conditioned media altering the expression of hundreds of host epithelial genes linked to immune response, cell adhesion, cell cycle, and development in IECs *in vitro* (Hughes et al., 2017; Guo et al., 2015). However, the direct impact of bifidobacterial-associated metabolites on these responses would require further studies to confirm metabolic activity of *B. breve* within the small intestine (via transcriptomics and metabolomics), although daily

supplementation with live bacteria may also provide a source of these metabolites in our model. Interestingly, certain *Bifidobacterium* and *Lactobacillus* strains that have been heat killed have also been shown to induce host responses, indicating that surface structures alone may play a role in downstream effects (Pique et al., 2019). All but two of the 37 differentially expressed stem cell marker genes were up-regulated in the presence of *B. breve* UCC2003, indicating an activating effect resulting in increased pluripotency of stem cells, increased quantity of stem cells, and/or an increased quantity of semi-differentiated cells. Single-cell sequencing of IECs could be used to further investigate this finding. Thirty-two TFs were predicted to regulate these stem cell signature genes, providing possible targets for future investigation of the mechanisms underlying these responses. Functional analysis of the stem cell signature genes and their regulators suggests that *B. breve* increases pluripotency of stem cells and/or semi-differentiated epithelial cells through WNT signaling and nuclear hormone signaling (Jeong and Mangelsdorf, 2009). Furthermore, the overrepresentation of the process “RUNX1 regulates transcription of genes involved in differentiation of HSCs” indicates a possible role for histone methylation in response to *B. breve* UCC2003 (Imperato et al., 2015). Further determination of host and bacterial metabolome and proteome after *B. breve* exposure may allow identification of the specific underlying molecular mechanisms (Guo et al., 2015).

In conclusion, *B. breve* UCC2003 plays a central role in orchestrating global neonatal IEC gene responses in a distinct manner as shown in our murine model, modulating genes involved in epithelial barrier development, and driving universal transcriptomic alteration that facilitates cell replication, differentiation, and growth, particularly within the stem cell compartment. This study enhances our overall understanding of the benefits of specific early life microbiota members in intestinal epithelium development, with prospective avenues to probe further health-promoting mechanisms of *Bifidobacterium* in humans. Further work exploring time-dependent transcriptional responses and impact of other *Bifidobacterium* species and strains (and use of mutants and transcriptionally active strains as positive controls), in tandem with metabolomic and proteomic approaches, is required to advance our understanding on the key host pathways and bifidobacterial molecules governing development and maturation of the intestinal barrier during the early life window. Nevertheless, further clinical studies would be essential to explore if these responses and findings are similar to those observed in humans.

Limitations of the Study

As we only observed low relative abundance of *Bifidobacterium* in our control neonatal animals this may suggest that induction of responses may be linked to the introduction of a new microbiota member (i.e., *B. breve* UCC2003), therefore results should be carefully interpreted. However, we did not observe associated global transcriptional inflammatory immune changes that would be expected if this was the case, but rather global changes in barrier function transcripts and pathways. Furthermore, *Bifidobacterium* has previously been isolated from C57BL/6 mice (including from our mouse colony), and therefore appears to be a resident rodent gut microbiota member, although it is found at varying abundances in different animal units and suppliers (Grimm et al., 2015; Hughes et al., 2020). Indeed, one particular study has shown that high levels of resident *Bifidobacterium* in mice directly correlated with improved immune responses to cancer immunotherapies (Sivan et al., 2015). In addition, we did not explore if *B. breve* UCC2003 is potentially driving more nuanced microbe-microbe interactions, and that, indirectly, these may also be stimulating IEC responses. Therefore, further studies probing these aspects in more detail, and comparing other *Bifidobacterium* strains, to compare and contrast responses, would be of interest.

B. breve UCC2003 is a model strain that was previously isolated from the stool of a breast-fed infant (National Collection of Industrial Food and Marine Bacteria, 2020, Sheehan et al., 2007). Although a human-associated strain, it has not been used in clinical studies, so directly extrapolating to human-specific settings should be cautiously considered. Further large-scale clinical studies would be required to confirm any positive strain-level impacts; however, in-depth analysis of, e.g., small IECs would be unethical in a healthy infant cohort, which emphasizes the importance of preclinical models.

Previous studies have shown that this strain can efficiently colonize (long term) the mouse gastrointestinal tract; however, we could not confirm this in our short-term, daily supplementation study (Cronin et al., 2008, O’Connell Motherway et al., 2011). Therefore the IEC responses observed may occur as a result of transient interactions with *B. breve* UCC2003 as it passes through the small intestine. Nevertheless, although at lower levels ($\sim 10^5$ CFU/g), we did observe viable *B. breve* UCC2003 in the small intestine, linking to our subsequent observations of significant impacts on the IEC transcriptome from this intestinal region.

Very-low-abundance microbiota members (<2% relative abundance), including *Streptococcus*, *Ruminococcus*, *Prevotella*, and *Coprococcus*, were significantly reduced in relative abundance compared with controls, raising the question whether supplementation of *Bifidobacterium* could have reduced these taxa. Regrettably, we could not determine if this is a bifidobacterial effect due to the lack of longitudinal samples, and we did not quantify bacterial titers, which is an important consideration for future work. We also did not profile microbial community composition within the small intestines, which is known to differ from fecal samples.

Resource Availability

Lead Contact

Further information and requests for resources and reagents should be directed to and will be fulfilled by the Lead Contact, Lindsay J. Hall (Lindsay.Hall@quadram.ac.uk).

Materials Availability

This study did not generate new unique reagents.

Data and Code Availability

The code generated for RNA-seq analysis during this study is available at GitHub <https://github.com/raymondkiu/Bifidobacterium-IEC-transcriptomics>. The accession number for the raw sequencing reads (both RNA-seq and 16S rRNA amplicon sequencing) reported in this paper is European Nucleotide Archive (ENA): PRJEB36661.

METHODS

All methods can be found in the accompanying [Transparent Methods supplemental file](#).

SUPPLEMENTAL INFORMATION

Supplemental Information can be found online at <https://doi.org/10.1016/j.isci.2020.101336>.

ACKNOWLEDGMENTS

This research was supported in part by the Norwich Bioscience Institutes (NBI) Computing infrastructure for Science (CiS) group through the provision of a High-Performance Computing (HPC) Cluster. L.J.H. is funded by a Wellcome Trust Investigator award (100974/C/13/Z) and together with T.K. by a BBSRC ISP grant for Gut Microbes and Health BB/R012490/1 and its constituent project(s), BBS/E/F/000PR10353 and BBS/E/F/000PR10355. T.K. is also funded by the Genomics for Food security CSP grant from the BBSRC (BB/CSP17270/1). A.T. is supported by the BBSRC Norwich Research Park Biosciences Doctoral Training Partnership (grant BB/M011216/1). D.v.S. is supported by Science Foundation Ireland (SFI/12/RC/2273-P1 and SFI/12/RC/2273-P2).

AUTHOR CONTRIBUTIONS

Conceptualization, R.K., L.C.H., and L.J.H.; Methodology, R.K., A.T., L.C.H., and L.J.H.; Software, R.K., A.T., and S.C.; Validation, R.K., A.T., T.K., and L.J.H.; Formal analysis, R.K. and A.T.; Investigation, R.K., A.T., L.C.H., and C.L.; Resources, S.C.; Data Curation, R.K.; Writing – Original Draft Preparation, R.K., A.T., and L.J.H.; Writing – Review and Editing, R.K., A.T., D.v.S., T.K., and L.J.H.; Visualization, R.K. and A.T.; Supervision, T.K. and L.J.H.; Project Administration, R.K.; Funding Acquisition, T.K., D.v.S., and L.J.H.

DECLARATION OF INTERESTS

The authors declare no competing interests.

Received: March 30, 2020

Revised: June 5, 2020

Accepted: June 30, 2020

Published: July 24, 2020

REFERENCES

Arrieta, M.C., Stiemsma, L.T., Amenogbe, N., Brown, E.M., and Finlay, B. (2014). The intestinal microbiome in early life: health and disease. *Front. Immunol.* 5, 427.

Baucells, B.J., Mercadal Hally, M., Alvarez Sanchez, A.T., and Figueras Aloy, J. (2016). Probiotic associations in the prevention of necrotising enterocolitis and the reduction of late-onset sepsis and neonatal mortality in preterm infants under 1,500g: a systematic review. *An. Pediatr. (Barc.)* 85, 247–255.

Chernyavsky, A.I., Arredondo, J., Karlsson, E., Wessler, I., and Grando, S.A. (2005). The Ras/Raf-1/MEK1/ERK signaling pathway coupled to integrin expression mediates cholinergic regulation of keratinocyte directional migration. *J. Biol. Chem.* 280, 39220–39228.

Cronin, M., Sleator, R.D., Hill, C., Fitzgerald, G.F., and van Sinderen, D. (2008). Development of a luciferase-based reporter system to monitor *Bifidobacterium breve* UCC2003 persistence in mice. *BMC Microbiol.* 8, 161.

Derrien, M., Alvarez, A.S., and de Vos, W.M. (2019). The gut microbiota in the first decade of life. *Trends Microbiol.* 27, 997–1010.

Din, A.U., Hassan, A., and Zhu, Y. (2020). Inhibitory effect of *Bifidobacterium Bifidum* ATCC29521 on colitis and its mechanism. *J. Nutr. Biochem.* 79, 108353.

Dominguez-Bello, M.G., Costello, E.K., Contreras, M., Magris, M., Hidalgo, G., Fierer, N., and Knight, R. (2010). Delivery mode shapes the acquisition and structure of the initial microbiota across multiple body habitats in newborns. *Proc. Natl. Acad. Sci. U S A* 107, 11971–11975.

Edelblum, K.L., and Turner, J.R. (2009). The tight junction in inflammatory disease: communication breakdown. *Curr. Opin. Pharmacol.* 9, 715–720.

Ewaschuk, J.B., Diaz, H., Meddings, L., Diederichs, B., Dmytrash, A., Backer, J., Looijer-van Langen, M., and Madsen, K.L. (2008). Secreted bioactive factors from *Bifidobacterium infantis* enhance epithelial Cell barrier function. *Am. J. Physiol. Gastrointest. Liver Physiol.* 295, G1025–G1034.

Favier, C., Neut, C., Mizon, C., Cortot, A., Colombel, J.F., and Mizon, J. (1997). Fecal beta-D-galactosidase production and *Bifidobacteria* are decreased in Crohn's disease. *Dig. Dis. Sci.* 42, 817–822.

Fukuda, S., Toh, H., Taylor, T.D., Ohno, H., and Hattori, M. (2012). Acetate-producing bifidobacteria protect the host from enteropathogenic infection via carbohydrate transporters. *Gut Microbes* 3, 449–454.

Furie, E., Macfarlane, S., Kennedy, A., Cummings, J.H., Walsh, S.V., O'neil, D.A., and Macfarlane, G.T. (2005). Synbiotic therapy (*Bifidobacterium longum*/Synergy 1) initiates resolution of inflammation in patients with active ulcerative colitis: a randomised controlled pilot trial. *Gut* 54, 242–249.

Gann, R.N. (2010). Host Signaling Response to Adhesion of *Bifidobacterium infantis*, All Graduate Theses and Dissertations Thesis (Utah State University).

Garcia-Alonso, L., Holland, C.H., Ibrahim, M.M., Turei, D., and Saez-Rodriguez, J. (2019). Benchmark and integration of resources for the estimation of human transcription factor activities. *Genome Res.* 29, 1363–1375.

Grimm, V., Radulovic, K., and Riedel, C.U. (2015). Colonization of C57BL/6 mice by a potential probiotic *Bifidobacterium bifidum* strain under germ-free and specific pathogen-free conditions and during experimental colitis. *PLoS One* 10, e0139935.

Groschwitz, K.R., and Hogan, S.P. (2009). Intestinal barrier function: molecular regulation and disease pathogenesis. *J. Allergy Clin. Immunol.* 124, 3–20, quiz 21–2.

Guo, S., Guo, Y., Ergun, A., Lu, L., Walker, W.A., and Ganguli, K. (2015). Secreted metabolites of *Bifidobacterium infantis* and *Lactobacillus acidophilus* protect immature human enterocytes from IL-1beta-induced inflammation: a transcription profiling analysis. *PLoS One* 10, e0124549.

Haber, A.L., Biton, M., Rogel, N., Herbst, R.H., Shekhar, K., Smillie, C., Burgin, G., Delorey, T.M., Howitt, M.R., Katz, Y., Tirosh, I., Beyaz, S., Dionne, D., and Zhang, M. (2017). A single-cell survey of the small intestinal epithelium. *Nature* 551, 333–339.

Harburger, D.S., and Calderwood, D.A. (2009). Integrin signalling at a glance. *J. Cell Sci.* 122, 159–163.

Hildebrand, H., Malmberg, P., Asking, J., Ekblom, A., and Montgomery, S.M. (2008). Early-life exposures associated with antibiotic use and risk of subsequent Crohn's disease. *Scand. J. Gastroenterol.* 43, 961–966.

Holland, C.H., Szalai, B., and Saez-Rodriguez, J. (2019). Transfer of regulatory knowledge from human to mouse for functional genomics analysis. *Biochim. Biophys. Acta Gene Regul. Mech.* 1863, 194431.

Hsieh, C.Y., Osaka, T., Moriyama, E., Date, Y., Kikuchi, J., and Tsuneda, S. (2015). Strengthening of the intestinal epithelial tight junction by *Bifidobacterium bifidum*. *Physiol. Rep.* 3, e12327.

Hughes, K.R., Harnisch, L.C., Alcon-Giner, C., Mitra, S., Wright, C.J., Ketskemety, J., van Sinderen, D., Watson, A.J., and Hall, L.J. (2017). *Bifidobacterium breve* reduces apoptotic epithelial cell shedding in an exopolysaccharide and MyD88-dependent manner. *Open Biol.* 7, 160155.

Hughes, K.R., Schofield, Z., Dalby, M.J., Caim, S., Chalklen, L., Bernuzzi, F., Alcon-Giner, C., Le Gall, G., Watson, A.J.M., and Hall, L.J. (2020). The early life microbiota protects neonatal mice from pathological small intestinal epithelial cell shedding. *FASEB J.* 34, 7075–7088.

Imperato, M.R., Cauchy, P., Obier, N., and Bonifer, C. (2015). The RUNX1-PU.1 axis in the control of hematopoiesis. *Int. J. Hematol.* 101, 319–329.

Jacobs, S.E., Tobin, J.M., Opie, G.F., Donath, S., Tabrizi, S.N., Pirota, M., Morley, C.J., Garland, S.M., and Proprems Study, G. (2013). Probiotic effects on late-onset sepsis in very preterm infants: a randomized controlled trial. *Pediatrics* 132, 1055–1062.

Jeong, Y., and Mangelsdorf, D.J. (2009). Nuclear receptor regulation of stemness and stem cell differentiation. *Exp. Mol. Med.* 41, 525–537.

Kronman, M.P., Zautis, T.E., Haynes, K., Feng, R., and Coffin, S.E. (2012). Antibiotic exposure and IBD development among children: a population-based cohort study. *Pediatrics* 130, e794–803.

Krug, S.M., Schulzke, J.D., and Fromm, M. (2014). Tight junction, selective permeability, and related diseases. *Semin. Cell Dev. Biol.* 36, 166–176.

Lawson, M.A.E., O'neill, I.J., Kujawska, M., Gowrinadh Javadi, S., Wijeyesekera, A., Flegg, Z., Chalklen, L., and Hall, L.J. (2020). Breast milk-derived human milk oligosaccharides promote *Bifidobacterium* interactions within a single ecosystem. *ISME J.* 14, 635–648.

Lewis, M.C., Merrifield, C.A., Berger, B., Cloarec, O., Duncker, S., Mercenier, A., Nicholson, J.K., Holmes, E., and Bailey, M. (2017). Early intervention with *Bifidobacterium lactis* NCC2818 modulates the host-microbe interface independent of the sustained changes induced by the neonatal environment. *Sci. Rep.* 7, 5310.

Li, L., Zhao, G.D., Shi, Z., Qi, L.L., Zhou, L.Y., and Fu, Z.X. (2016). The Ras/Raf/MEK/ERK signaling pathway and its role in the occurrence and development of HCC. *Oncol. Lett.* 12, 3045–3050.

Ling, X., Linglong, P., Weixia, D., and Hong, W. (2016). Protective effects of *Bifidobacterium* on intestinal barrier function in LPS-induced enterocyte barrier injury of caco-2 monolayers and in a rat NEC model. *PLoS One* 11, e0161635.

Liu, C., Zhang, Z.Y., Dong, K., and Guo, X.K. (2010). Adhesion and immunomodulatory effects of *Bifidobacterium lactis* HN019 on intestinal epithelial cells INT-407. *World J. Gastroenterol.* 16, 2283–2290.

Mikami, K., Kimura, M., and Takahashi, H. (2012). Influence of maternal bifidobacteria on the development of gut bifidobacteria in infants. *Pharmaceuticals (Basel)* 5, 629–642.

Mosher, D.F., Fogerty, F.J., Chernousov, M.A., and Barry, E.L. (1991). Assembly of fibronectin into extracellular matrix. *Ann. N. Y Acad. Sci.* 614, 167–180.

Nagpal, R., Kurakawa, T., Tsuji, H., Takahashi, T., Kawashima, K., Nagata, S., Nomoto, K., and Yamashiro, Y. (2017). Evolution of gut *Bifidobacterium* population in healthy Japanese infants over the first three years of life: a quantitative assessment. *Sci. Rep.* 7, 10097.

National Collection of Industrial Food and Marine Bacteria (NCIMB) (2020). NCIMB 8807 General Info (Aberdeen).

Ng, S.C., Benjamin, J.L., McCarthy, N.E., Hedin, C.R., Koutsoumpas, A., Plamondon, S., Price, C.L., Hart, A.L., Kamm, M.A., Forbes, A., Knight, S.C., Lindsay, J.O., Whelan, K., and Stagg, A.J.

- (2011). Relationship between human intestinal dendritic cells, gut microbiota, and disease activity in Crohn's disease. *Inflamm. Bowel Dis.* 17, 2027–2037.
- Nusse, R. (2008). Wnt signaling and stem cell control. *Cell Res.* 18, 523–527.
- O'Connell Motherway, M., Houston, A., O'callaghan, G., Reunanen, J., O'brien, F., O'driscoll, T., Casey, P.G., de Vos, W.M., van Sinderen, D., and Shanahan, F. (2019). A Bifidobacterial pilus-associated protein promotes colonic epithelial proliferation. *Mol. Microbiol.* 111, 287–301.
- O'Connell Motherway, M., Zomer, A., Leahy, S.C., Reunanen, J., Bottacini, F., Claesson, M.J., O'brien, F., Flynn, K., Casey, P.G., Munoz, J.A., Kearney, B., Houston, A.M., and O'mahony, C. (2011). Functional genome analysis of Bifidobacterium breve UCC2003 reveals type IVb tight adherence (Tad) pili as an essential and conserved host-colonization factor. *Proc. Natl. Acad. Sci. U S A* 108, 11217–11222.
- O'Neill, I., Schofield, Z., and Hall, L.J. (2017). Exploring the role of the microbiota member Bifidobacterium in modulating immune-linked diseases. *Emerg. Top. Life Sci.* 1, 333–349.
- Pan, W.H., Sommer, F., Falk-Paulsen, M., Ulas, T., Best, P., Fazio, A., Kachroo, P., Luzius, A., Jentsch, M., Rehman, A., Muller, F., Lengauer, T., Walter, J., Kunzel, S., and Baines, J.F. (2018). Exposure to the gut microbiota drives distinct methylome and transcriptome changes in intestinal epithelial cells during postnatal development. *Genome Med.* 10, 27.
- Patole, S.K., Rao, S.C., Keil, A.D., Nathan, E.A., Doherty, D.A., and Simmer, K.N. (2016). Benefits of Bifidobacterium breve M-16V supplementation in preterm neonates - a retrospective cohort study. *PLoS One* 11, e0150775.
- Philippe, D., Heupel, E., Blum-Sperisen, S., and Riedel, C.U. (2011). Treatment with Bifidobacterium bifidum 17 partially protects mice from Th1-driven inflammation in a chemically induced model of colitis. *Int. J. Food Microbiol.* 149, 45–49.
- Pique, N., Berlanga, M., and Minana-Galbis, D. (2019). Health benefits of heat-killed (Tyndallized) probiotics: an overview. *Int. J. Mol. Sci.* 20, 2534.
- Plantinga, T.S., van Maren, W.W., van Bergenhenegouwen, J., Hameetman, M., Nierkens, S., Jacobs, C., de Jong, D.J., Joosten, L.A., Van't Land, B., Garssen, J., Adema, G.J., and Netea, M.G. (2011). Differential Toll-like receptor recognition and induction of cytokine profile by Bifidobacterium breve and Lactobacillus strains of probiotics. *Clin. Vaccin. Immunol.* 18, 621–628.
- Plaza-Diaz, J., Gomez-Llorente, C., Fontana, L., and Gil, A. (2014). Modulation of immunity and inflammatory gene expression in the gut, in inflammatory diseases of the gut and in the liver by probiotics. *World J. Gastroenterol.* 20, 15632–15649.
- Plummer, E.L., Bulach, D.M., Murray, G.L., Jacobs, S.E., Tabrizi, S.N., Garland, S.M., and Proprems Study, G. (2018). Gut microbiota of preterm infants supplemented with probiotics: sub-study of the ProPrems trial. *BMC Microbiol.* 18, 184.
- Qin, J., Vinogradova, O., and Plow, E.F. (2004). Integrin bidirectional signaling: a molecular view. *PLoS Biol.* 2, e169.
- Riedel, C.U., Foata, F., Philippe, D., Adolfsson, O., Eikmanns, B.J., and Blum, S. (2006). Anti-inflammatory effects of bifidobacteria by inhibition of LPS-induced NF-kappaB activation. *World J. Gastroenterol.* 12, 3729–3735.
- Robertson, C., Savva, G.M., Clapuci, R., Jones, J., Maimouni, H., Brown, E., Minocha, A., Hall, L.J., and Clarke, P. (2020). Incidence of necrotising enterocolitis before and after introducing routine prophylactic Lactobacillus and Bifidobacterium probiotics. *Arch. Dis. Child. Fetal Neonatal Ed.* 105, 380–386.
- Shaw, S.Y., Blanchard, J.F., and Bernstein, C.N. (2010). Association between the use of antibiotics in the first year of life and pediatric inflammatory bowel disease. *Am. J. Gastroenterol.* 105, 2687–2692.
- Sheehan, V.M., Sleator, R.D., Hill, C., and Fitzgerald, G.F. (2007). Improving gastric transit, gastrointestinal persistence and therapeutic efficacy of the probiotic strain Bifidobacterium breve UCC2003. *Microbiology* 153, 3563–3571.
- Shirazi, T., Longman, R.J., Corfield, A.P., and Probert, C.S. (2000). Mucins and inflammatory bowel disease. *Postgrad. Med. J.* 76, 473–478.
- Sivan, A., Corrales, L., Hubert, N., Williams, J.B., Aquino-Michaels, K., Earley, Z.M., Benyamin, F.W., Lei, Y.M., Jabri, B., Alegre, M.L., Chang, E.B., and Gajewski, T.F. (2015). Commensal Bifidobacterium promotes antitumor immunity and facilitates anti-PD-L1 efficacy. *Science* 350, 1084–1089.
- Srutkova, D., Schwarzer, M., Hudcovic, T., Zakostelska, Z., Drab, V., Spanova, A., Rittich, B., Kozakova, H., and Schabussova, I. (2015). Bifidobacterium longum CCM 7952 promotes epithelial barrier function and prevents acute DSS-induced colitis in strictly strain-specific manner. *PLoS One* 10, e0134050.
- Steed, H., Macfarlane, G.T., Blackett, K.L., Bahrami, B., Reynolds, N., Walsh, S.V., Cummings, J.H., and Macfarlane, S. (2010). Clinical trial: the microbiological and immunological effects of synbiotic consumption - a randomized double-blind placebo-controlled study in active Crohn's disease. *Aliment. Pharmacol. Ther.* 32, 872–883.
- Stewart, C.J., Ajami, N.J., O'brien, J.L., Hutchinson, D.S., Smith, D.P., Wong, M.C., Ross, M.C., Lloyd, R.E., Doddapaneni, H., Metcalf, G.A., Muzny, D., Gibbs, R.A., Vatanen, T., Huttenhower, C., Xavier, R.J., and Rewers, M. (2018). Temporal development of the gut microbiome in early childhood from the TEDDY study. *Nature* 562, 583–588.
- Thoo, L., Noti, M., and Krebs, P. (2019). Keep calm: the intestinal barrier at the interface of peace and war. *Cell Death Dis.* 10, 849.
- Tomosada, Y., Villena, J., Murata, K., Chiba, E., Shimazu, T., Aso, H., Iwabuchi, N., Xiao, J.Z., Saito, T., and Kitazawa, H. (2013). Immunoregulatory effect of bifidobacteria strains in porcine intestinal epithelial cells through modulation of ubiquitin-editing enzyme A20 expression. *PLoS One* 8, e59259.
- Turrone, F., Taverniti, V., Ruas-Madiedo, P., Duranti, S., Guglielmetti, S., Lugli, G.A., Gioiosa, L., Palanza, P., Margolles, A., van Sinderen, D., and Ventura, M. (2014). Bifidobacterium bifidum PRL2010 modulates the host innate immune response. *Appl. Environ. Microbiol.* 80, 730–740.
- Van der Sluis, M., de Koning, B.A., de Bruijn, A.C., Velcich, A., Meijerink, J.P., van Goudoever, J.B., Buller, H.A., Dekker, J., van Seuningen, I., Renes, I.B., and Einerhand, A.W. (2006). Muc2-deficient mice spontaneously develop colitis, indicating that MUC2 is critical for colonic protection. *Gastroenterology* 131, 117–129.
- Zheng, B., van Bergenhenegouwen, J., Overbeek, S., van de Kant, H.J., Garssen, J., Folkerts, G., Vos, P., Morgan, M.E., and Kraneveld, A.D. (2014). Bifidobacterium breve attenuates murine dextran sodium sulfate-induced colitis and increases regulatory T cell responses. *PLoS One* 9, e95441.
- Zuo, L., Yuan, K.T., Yu, L., Meng, Q.H., Chung, P.C., and Yang, D.H. (2014). Bifidobacterium infantis attenuates colitis by regulating T cell subset responses. *World J. Gastroenterol.* 20, 18316–18329.

iScience, Volume 23

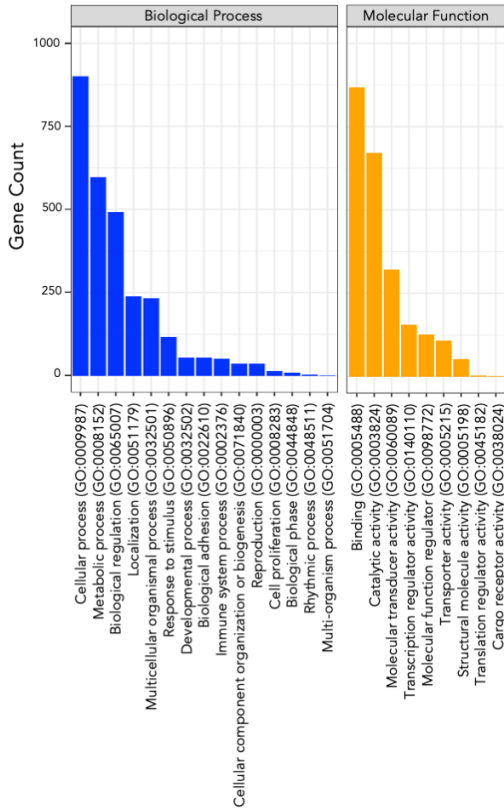
Supplemental Information

***Bifidobacterium breve* UCC2003 Induces a Distinct Global Transcriptomic Program in Neonatal Murine Intestinal Epithelial Cells**

Raymond Kiu, Agatha Treveil, Lukas C. Harnisch, Shabhonam Caim, Charlotte Leclaire, Douwe van Sinderen, Tamas Korcsmaros, and Lindsay J. Hall

SUPPLEMENTAL FIGURE

A



B

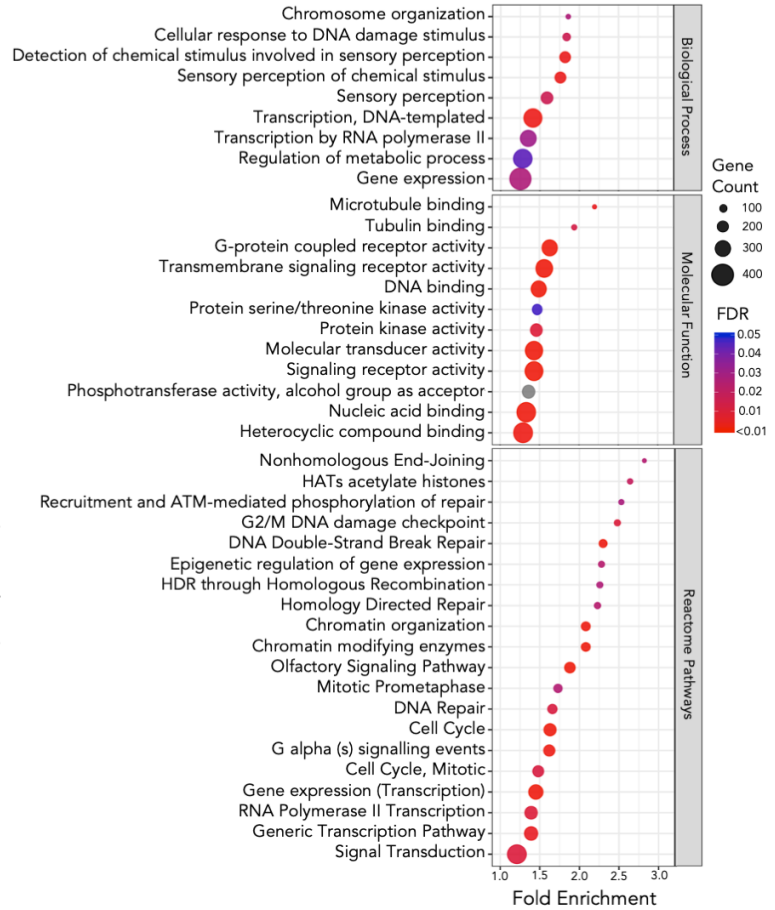


Figure S1. Functional analysis on differentially expressed genes. Related to Figure 4.

(A) Panther Slim GO-term major categories of significantly up-regulated genes ($n=3,996$). Related to Table S7 and Table S8.

(B) Functional and pathway enrichment analysis on significantly up-regulated genes (Panther Slim GO-term). Only top 20 FDR-ranked enriched pathways (Reactome pathways) are shown. Statistical significance cut-offs: $FDR < 0.05$. Statistical significance: Fisher's Exact Test. Fold Enrichment was calculated against all expressed genes in IECs as the background ($n=21,537$). Related to Table S5, Table S6 and Table S9.

SUPPLEMENTAL TABLES

Gene	Ensembl ID	Chromosome	Description/ Putative function	Biological process (GO)
<i>Gm27149</i>	ENSMUSG00000098426	7	Unknown	Unknown
<i>Ccnb1ip1</i>	ENSMUSG00000071470	14	Cyclin B1 interacting protein 1	Cell differentiation, Cellular component organisation, Protein metabolic process
<i>Gm10359</i>	ENSMUSG00000094708	5	glyceraldehyde-3-phosphate dehydrogenase pseudogene	Unknown
<i>Gm12671</i>	ENSMUSG00000095937	4	glyceraldehyde-3-phosphate dehydrogenase pseudogene	Unknown
<i>Gm48216</i>	ENSMUSG00000114367	13	Unknown	Unknown
<i>Gm17131</i>	ENSMUSG00000085328	5	Unknown	Unknown
<i>Tmem72</i>	ENSMUSG00000048108	6	transmembrane protein 72	Unknown
<i>Ccdc107</i>	ENSMUSG00000028461	4	coiled-coil domain containing 107	Unknown
CR936839.3	ENSMUSG00000111855	Unknown	Unknown	Unknown
<i>Hist1h4b</i>	ENSMUSG00000069266	13	H4 clustered histone 2	Cell differentiation, Cellular component organisation, Immune system process, system development
<i>Gm48836</i>	ENSMUSG00000113523	12	Unknown	Unknown
<i>Gm42669</i>	ENSMUSG00000106631	5	Unknown	Unknown
<i>Gprin3</i>	ENSMUSG00000045441	6	GPRIN family member 3	Unknown
<i>Fgd4</i>	ENSMUSG00000022788	16	FYVE, RhoGEF and PH domain containing 4	Cellular component of organisation, Protein metabolic process, Response to stimulus, Signaling
<i>D10Wsu102e</i>	ENSMUSG00000020255	10	DNA segment, Chr 10, Wayne State University 102, expressed	Unknown
<i>Gm20594</i>	ENSMUSG00000096887	6	Unknown	Cell death, Response to stimulus, Signaling
<i>Vps13b</i>	ENSMUSG00000037646	15	vacuolar protein sorting 13B	Establishment of localisation
<i>Gm48366</i>	ENSMUSG00000113523	12	Unknown	Unknown
<i>Gm48054</i>	ENSMUSG00000113921	13	Unknown	Unknown
<i>Naip6</i>	ENSMUSG00000078942	13	NLR family, apoptosis inhibitory protein 6	Cell death, Immune system process, Response to stimulus

Table S3. Annotation of top 20 significantly up-regulated genes. Related to Figure 4.

Gene	Ensembl ID	Chromosome	Description/ Putative function	Biological process (GO)
<i>Gm7849</i>	ENSMUSG00000079114	8	Defensin	Immune system process, response to stimulus
<i>Rps27rt</i>	ENSMUSG00000050621	9	ribosomal protein S27, retrogene	Unknown
<i>Gm6158</i>	ENSMUSG00000090381	14	Unknown	Unknown
<i>mt-Co2</i>	ENSMUSG00000064354	MT	mitochondrially encoded cytochrome c oxidase II	Carbohydrate derivative metabolism, cell death
<i>Gm3650</i>	ENSMUSG00000097891	18	Unknown	Unknown
<i>Gm5831</i>	ENSMUSG00000111133	9	Unknown	Unknown
<i>Gm7331</i>	ENSMUSG00000059461	X	Unknown	Unknown
<i>Polr3h</i>	ENSMUSG00000022476	15	polymerase (RNA) III (DNA directed) polypeptide H	Immune system process, response to stimulus
<i>Gm14698</i>	ENSMUSG00000071748	X	Unknown	Unknown
<i>Ftl1-ps1</i>	ENSMUSG00000062382	13	erritin light polypeptide 1	Unknown
<i>Rps16</i>	ENSMUSG00000037563	7	ribosomal protein S16	Protein metabolic process, response to stimulus
<i>Mt2</i>	ENSMUSG00000031762	8	metallothionein 2	Homeostatic process, response to stimulus, signaling
<i>Mt1</i>	ENSMUSG00000031765	8	metallothionein 1	Cell death, homeostatic process, response to stimulus, signaling
<i>Hba-a1</i>	ENSMUSG00000069919	11	hemoglobin alpha	Cell differentiation, homeostatic process, immune system process, response to stimulus, signaling, system development
<i>Hbb-bt</i>	ENSMUSG00000073940	7	hemoglobin, beta adult t chain	Unknown
<i>Rps2-ps10</i>	ENSMUSG00000091957	18	ribosomal protein S2	Unknown
<i>Gpx3</i>	ENSMUSG00000018339	11	glutathione peroxidase 3	Response to stimulus
<i>Smcp</i>	ENSMUSG00000074435	3	sperm mitochondria-associated cysteine-rich protei	Unknown
<i>Gm49384</i>	ENSMUSG00000113786	12	Predicted gene	Unknown
<i>Gm7336</i>	ENSMUSG00000078636	7	Predicted gene	Unknown

Table S4. Annotation of top 20 significantly down-regulated genes. Related to Figure 4.

GO Biological Process	Gene Count	Fold Enrichment	FDR
Transcription, DNA-templated	252	1.41	1.15E-03
Detection of chemical stimulus involved in sensory perception	97	1.82	1.92E-03
Sensory perception of chemical stimulus	98	1.76	1.97E-03
Cellular response to DNA damage stimulus	66	1.84	1.54E-02
Sensory perception	111	1.59	1.57E-02
Gene expression	350	1.25	2.66E-02
Chromosome organization	57	1.86	2.66E-02
Transcription by RNA polymerase II	193	1.35	3.09E-02
Regulation of metabolic process	262	1.28	4.48E-02

Table S5. GO Biological Process enrichment analysis in up-regulated DEGs. Related to Figure 4 and Figure S1.

GO Molecular Functions	Gene Count	Fold Enrichment	FDR
Transmembrane signaling receptor activity	279	1.56	5.07E-08
G-protein coupled receptor activity	224	1.63	8.61E-08
Molecular transducer activity	321	1.43	1.76E-06
Signaling receptor activity	302	1.43	4.06E-06
DNA binding	225	1.49	1.20E-05
Nucleic acid binding	344	1.33	1.14E-04
Heterocyclic compound binding	352	1.29	7.08E-04
Microtubule binding	43	2.2	3.01E-03
Protein kinase activity	133	1.46	7.97E-03
Tubulin binding	45	1.94	1.24E-02
Protein serine/threonine kinase activity	94	1.47	4.74E-02
Phosphotransferase activity, alcohol group as acceptor	144	1.36	5.04E-02

Table S6. GO Molecular Functions enrichment analysis in up-regulated DEGs. Related to Figure 4 and Figure S1.

Biological Process	Genes	Percentage
cellular process (GO:0009987)	901	31.70%
metabolic process (GO:0008152)	597	21.00%
biological regulation (GO:0065007)	492	17.30%
localization (GO:0051179)	239	8.40%
multicellular organismal process (GO:0032501)	233	8.20%
response to stimulus (GO:0050896)	117	4.10%
developmental process (GO:0032502)	55	1.90%
biological adhesion (GO:0022610)	55	1.90%
immune system process (GO:0002376)	52	1.80%
cellular component organization or biogenesis (GO:0071840)	37	1.30%
reproduction (GO:0000003)	37	1.30%
cell proliferation (GO:0008283)	15	0.50%
biological phase (GO:0044848)	10	0.40%
rhythmic process (GO:0048511)	4	0.10%
multi-organism process (GO:0051704)	2	0.10%

Table S7. GO Biological Process functional assignment to 3,996 upregulated genes. Related to Figure 4 and Figure S1.

Molecular Function	Genes	Percentage
binding (GO:0005488)	868	37.60%
catalytic activity (GO:0003824)	671	29.00%
molecular transducer activity (GO:0060089)	321	13.90%
transcription regulator activity (GO:0140110)	156	6.80%
molecular function regulator (GO:0098772)	127	5.50%
transporter activity (GO:0005215)	108	4.70%
structural molecule activity (GO:0005198)	53	2.30%
translation regulator activity (GO:0045182)	4	0.20%
cargo receptor activity (GO:0038024)	2	0.10%

Table S8. GO Molecular Function functional assignment to 3,996 upregulated genes. Related to Figure 4 and Figure S1.

Reactome Pathway	Gene Count	Fold Enrichment	FDR
Olfactory Signaling Pathway	108	1.88	3.20E-05
Cell Cycle	154	1.63	1.13E-04
Gene expression (Transcription)	238	1.45	1.18E-04
Chromatin organization	67	2.08	2.54E-04
Chromatin modifying enzymeS	67	2.08	2.82E-04
DNA Double-Strand Break Repair	51	2.3	4.19E-04
G alpha (s) signalling events	122	1.62	6.50E-04
RNA Polymerase II Transcription	202	1.39	3.06E-03
Generic Transcription Pathway	173	1.39	8.50E-03
Signal Transduction	461	1.21	8.98E-03
G2/M DNA damage checkpoint	29	2.48	9.07E-03
DNA Repair	77	1.66	1.06E-02
Cell Cycle, Mitotic	122	1.48	1.06E-02
HATs acetylate histones	23	2.64	1.85E-02
Epigenetic regulation of gene expression	28	2.28	2.38E-02
Homology Directed Repair	30	2.23	2.39E-02
Nonhomologous End-Joining	19	2.82	2.46E-02
Mitotic Prometaphase	58	1.73	2.48E-02
HDR through Homologous Recombination	29	2.26	2.63E-02
Recruitment and ATM-mediated phosphorylation of repair	22	2.53	2.78E-02

Table S9. Reactome pathway enrichment analysis in up-regulated DEGs. Related to Figure 4 and Figure S1.

Reactome Pathway	Gene Count	Fold Enrichment	FDR
Regulation of FZD by ubiquitination (R-MMU-4641263)	3	35.6	2.39E-02
Endogenous sterols (R-MMU-211976)	3	27.06	3.63E-02
Estrogen-dependent gene expression (R-MMU-9018519)	6	19.61	4.95E-04
ESR-mediated signaling (R-MMU-8939211)	6	18.04	4.69E-04
RUNX1 regulates transcription of genes involved in differentiation of HSCs (R-MMU-8939236)	4	14.78	3.41E-02
Signaling by Nuclear Receptors (R-MMU-9006931)	6	11.66	4.23E-03
Transcriptional regulation by RUNX1 (R-MMU-8878171)	6	9.73	9.64E-03
Generic Transcription Pathway (R-MMU-212436)	15	5.88	4.71E-05
RNA Polymerase II Transcription (R-MMU-73857)	15	5	1.89E-04
Gene expression (Transcription) (R-MMU-74160)	15	4.38	4.93E-04
Signal Transduction (R-MMU-162582)	19	2.37	3.65E-02

Table S12. Reactome pathway enrichment analysis of differentially expressed stem cell signature genes and their expressed regulators. Related to Figure 5.

TRANSPARENT METHODS

Animals

All animal experiments and related protocols were performed in accordance with the Animals (Scientific Procedures) Act 1986 (ASPA) under project licence (PPL: 80/2545) and personal licence (PIL: I68D4DCCF), approved by UK Home Office and University of East Anglia (UEA) FMH Research Ethics Committee. C57BL/6J two-week-old neonatal female mice ($n=10$) were housed in two separate cages with their mothers within UEA Disease Modelling Unit. Mice were euthanised via ASPA Schedule 1 protocol (CO₂ and cervical dislocation).

Bacterial culturing, inoculum preparation and CFU enumeration

B. breve UCC2003 (also known as NCIMB 8807) was streaked from frozen glycerol stocks onto autoclaved Reinforced Clostridial Agar (RCA) plates (Oxoid, UK) and incubated in an anaerobic chamber (miniMACS, Don Whitley Scientific) at 37°C for 48 h prior to picking single colonies for inoculation in prewarmed sterilised Reinforced Clostridial Medium (Oxoid, UK).

For preparation of gavage inoculums, 5 ml of inoculated broth was incubated overnight followed by sub-culturing into 5 ml De Man, Rogosa and Sharpe (MRS) medium (Oxoid). After an additional overnight incubation, another sub-culturing into 40 ml RCM was performed. Inoculums were prepared from cultures by 3 rounds of centrifugation at 3220 g for 10 min followed by three PBS washes before dilution in 4 ml (adult mice) or 2 ml (neonatal mice) sterile PBS. Bacterial concentration of inoculum was enumerated by plating serial dilutions in sterile PBS on RCA plates and enumerating colonies following two-day incubation to calculate CFU/ml.

Bacterial treatment and administration

Neonatal mice were orally gavaged with *B. breve* UCC2003 inoculations of 10⁸ CFU/ml in 50 µl every 24 h for 3 consecutive days. Control mice received oral gavages of sterile PBS. *B. breve* UCC2003 viable presence/transition through the gut was confirmed by collection of fresh faeces or intestinal content homogenised with 1 ml sterile PBS followed by serial-dilution plating in sterile PBS on RCA supplemented with 50 mg/L mupirocin and counting of colonies following two-day incubation to calculate CFU/mg.

Gut microbiota profiling by 16S rRNA amplicon sequencing and analysis

Genomic DNA extraction of mouse faecal samples on day 4 was performed with FastDNA Spin Kit for Soil (MP Biomedicals) following manufacturer's instructions and extending the bead-beating step to 3 min as described previously (Alcon-Giner et al., 2019). Extracted DNA was quantified, normalised and sequenced on Illumina MiSeq platform using a read length of 2 × 300 bp. After quality pre-filtering and removals of chimeras, sequencing reads were analysed using open-reference OTU clustering strategy (QIIME v1.9.1) to assign bacterial taxonomy based on SILVA_132 database (Quast et al., 2013). OTU tables in BIOM format was converted to genus counts in MEGAN6 and visualised using R library *ggplot2* as described previously (Kiu et al., 2019, Caporaso et al., 2010, Huson et al., 2016).

Tissue collection and isolation of small intestinal epithelial cells (IECs)

Upon tissue harvesting, 0.5 cm² sections of small intestines were collected in 200 µl RNAlater™ (Thermo Fisher Scientific) at the animal unit prior to IECs isolation (from fresh samples) via an adapted Weisser method as described below (Hughes et al., 2017). Sections of small intestines were placed in ice-cold PBS in 200 ml Duran bottles. Faecal matter was washed off by inverting 10 times in 0.154M NaCl and 1mM DTT. Liquid was drained and mucus layer removed through incubation of samples in 1.5mM KCl, 96mM NaCl, 27 mM Tri-sodium citrate, 8mM NaH₂PO₄ and 5.6mM Na₂HPO₄ for 15 min at 220 rpm and 37°C. IECs were separated from basal membrane by incubation in 1.5 mM EDTA and 0.5 mM DTT for 15 min at 200 rpm and 37 °C followed by shaking vigorously 20 times. IECs were collected from solution by centrifugation at 500 g for 10 min at 4 °C. Supernatant was then discarded and cell pellet resuspended in 3 ml of ice-cold PBS. Cell concentrations of

isolated IEC samples calculated by labelling dead cell with trypan blue at a 1:1 v/v ratio and enumeration of viable cells using a Neubauer haemocytometer on an inverted microscope (ID03, Zeiss).

RNA extraction and sequencing

RNA was extracted from IECs by adding a volume containing 2×10^6 cells in PBS to QIAshredder spin columns (QIAGEN) followed by centrifugation at 9,300 g for 1 min. Flow-through was mixed with 600 μ l RLT lysis buffer and used for subsequent RNA isolation. Homogenised samples in RLT buffer from IECs were processed by adding 700 μ l of 70% ethanol and mixing by pipetting. Samples were then added into RNeasy spin column and spun at 8,000 g for 15 s. Flow-through was discarded and process repeated until all of sample was filtered through column. Then 700 μ l of buffer RW1 was added to column and centrifuge at 8,000 g for 30 s. Again, flow through was discarded and filter placed in a new collection tube. To the filter, 500 μ l RPE was added and spun at 8,000 g for 30 s followed by discarding of flow through. An additional 500 μ l RPE was pipetted into column and centrifuged at 8,000 g for 2 min. Spin column was then placed in a new collection tube and centrifuged at 8,000 g for 2 min. Columns were transferred to a RNA low-bind Eppendorf tube and 30 μ l of RNase free water added to directly to the filter. After an incubation of 1 min at RT, sample was centrifuged at 8,000 g for 1 min and flow through containing RNA stored at -80°C .

Purified RNA was quantified, and quality controlled using RNA 6000 Nano kit on a 2100 Bioanalyser (Agilent). Only samples with RIN values above 8 were sequenced. RNA sequencing was performed at the Wellcome Trust Sanger Institute (Hinxton, UK) on paired-end 75 bp inserts on an Illumina HiSeq 2000 platform. Isolated RNA was processed by poly-A selection and/or Ribo-depletion.

Sequence pre-processing and Differential Gene Expression (DGE) analysis

Sequencing quality of raw FASTQ reads were assessed by FastQC software (v0.11.8). FASTQ reads were subsequently quality-filtered using fastp v0.20.0 with options `-q 10` (phred quality <10 was discarded) followed by merging reads into single read file for each sample (`merge-paired-reads.sh`) and rRNA sequence filtering via SortMeRNA v2.1 based on SILVA rRNA database optimised for SortMeRNA software (Chen et al., 2018, Kopylova et al., 2012). Filtered reads were then unmerged (`unmerge-paired-reads.sh`) and ready for transcript quantification.

Transcript mapping and quantification were performed using Kallisto v0.44.0 (Bray et al., 2016). Briefly, *Mus musculus* (C57BL/6 mouse) cDNA sequences (GRCm38.release-98_k31) were retrieved from Ensembl database and built into an index database with Kallisto utility `index` at default parameter that was used for following transcript mapping and abundance quantification via Kallisto utility `quant` at 100 bootstrap replicates (`-b 100`) (Zerbino et al., 2018).

DGE analysis was performed using R library Sleuth (v0.30.0) (Pimentel et al., 2017). Gene transcripts were mapped to individual genes using Ensembl BioMart database with Sleuth function `sleuth_prep` with option `gene_mode = TRUE`. Genes with an absolute $\log_2(\text{fold change}) > 1.0$ (based on Wald test statistics) and q value < 0.05 (or, FDR-adjusted p value; based on likelihood ratio test) were considered to be significantly regulated (Kinsella et al., 2011).

Functional annotation and enrichment analysis

Functional assignment and enrichment analysis was performed using PANTHER Classification System (Mi et al., 2019a). Briefly, for functional assignment analysis, a list of genes of interest in Ensembl IDs were supplied to the webserver to be mapped to the Mouse Genome Database (MGD) to generate functional classification on those genes of interest (Bult et al., 2019). For functional enrichment analysis, a gene list was supplied together with a background gene list in Ensembl IDs to Panther web server, then selected 'functional overrepresentation test' and chose a particular function class in the drop-down menu. Recommended by the database developers, Fisher's exact test and False Discovery Rate (FDR) correction were used to perform enrichment analysis (Mi et

al., 2019b). FDR <0.05 was used as the default cut-off for significant enrichment. Functional annotation of top 20 up/down-regulated genes was assigned manually via Ensembl and/or MGI (Mouse Genome Informatics) databases (Bult et al., 2019, Cunningham et al., 2019).

Network, cluster and signalling pathway analysis

A signalling network of all up-regulated DEGs and their first neighbours was built using all available biological signalling databases in the Cytoscape (v3.7.2) OmniPath app (v1, *Mus musculus*) (Turei et al., 2016, Shannon et al., 2003). Modules of highly connected genes within the signalling network were identified using the MCODE plug-in within Cytoscape (Bader and Hogue, 2003). Settings below were applied to obtain clusters in the network: degree cutoff = 3, haircut = true, fluff = false, node score cutoff = 0.5, k-core = 3 and max depth = 100.

The nodes of each individual module were tested for functional enrichment based on both Reactome and PANTHER annotations using PANTHER Classification System as described in previous sub-section '**Functional annotation and enrichment analysis**' (Mi and Thomas, 2009, Croft et al., 2011, Mi et al., 2019a).

Enrichment of cell type specific marker genes

Cell type signature gene sets for murine intestinal epithelial cells were obtained from Haber et al. (Haber et al., 2017). Both droplet and plate-based results were used. Gene symbols were converted to Ensembl IDs using db2db (Mudunuri et al., 2009). Hypergeometric significance calculations were applied to test the presence of cell type specific signatures in the list of differentially expressed genes using all expressed genes as the statistical background (normalised counts > 1 in ≥ 1 sample). Bonferroni multiple correction was applied and any corrected $p < 0.05$ was deemed significant. Genes with normalised counts > 1 in ≥ 1 sample per condition (*B. breve* UCC2003 treated or control) were used to identify cell type signature genes expressed per condition.

Key regulator analysis

All mouse transcription factor - target gene interactions with quality scores A-D were obtained from DoRothEA v2 via the OmniPath Cytoscape app (Garcia-Alonso et al., 2019, Shannon et al., 2003, Turei et al., 2016). A subnetwork was generated consisting of differentially expressed stem cell signature genes and all their upstream TFs which were expressed in the transcriptomics dataset (normalised counts > 1 in ≥ 1 sample). These TFs were further filtered for their relevance in the network. Here all expressed genes and their upstream expressed TFs were extracted from the DoRothEA network. A hypergeometric significance test was carried out on any node with degree ≥ 5 to determine if the proportion of connected nodes which are differentially expressed is higher than in the whole network. Any TF with $p < 0.05$ following Benjamini-Hochberg correction were deemed significant and used to filter the stem cell signature gene subnetwork. Network visualisation was carried out in Cytoscape (Shannon et al., 2003). Functional enrichment carried out against Reactome pathways as described in previous sub-sections.

Statistical analyses and graphing

Student t-tests were performed using Rv.3.6.0, details of which were provided in the results and figure legends (R Development Core Team, 2010). LDA statistical tests for microbiome analysis was performed via LefSe on Galaxy platform using default parameters (Segata et al., 2011, Jalili et al., 2020). PCA was performed via R library *ggfortify* function *autoplot* and *prcomp*, while Shannon diversity index was computed via R library *vegan* (Dixon, 2003, Tang et al., 2016, R Development Core Team, 2010). All other relevant statistical analyses (including enrichment analysis) were performed within specific software and details were provided in figure legends or as described in the previous sections.

All statistical graphs were either plotted using R library *ggplot2* or *Sleuth* (Wickham, 2016, Pimentel et al., 2017). Heatmaps were graphed using R library *gplots* function *heatmap.2* (Warnes et al., 2016).

Ethics approval

Animal experiments were performed under the UK Regulation of Animals (Scientific Procedures) Act of 1986. The project licence (PPL 80/2545) under which these studies were carried out was approved by the UK Home Office and the UEA Ethical Review Committee. Mice were sacrificed by CO₂ and cervical dislocation.

SUPPLEMENTAL REFERENCES

- ALCON-GINER, C., DALBY, M. J., CAIM, S., KETSKEMETY, J., SHAW, A., SIM, K., LAWSON, M., KIU, R., LECLAIRE, C., CHALKLEN, L., KUJAWSKA, M., MITRA, S., FARDUS-REID, F., BELTEKI, G., MCCOLL, K., SWANN, J. R., KROLL, J. S., CLARKE, P. & HALL, L. J. 2019. Microbiota supplementation with *Bifidobacterium* and *Lactobacillus* modifies the preterm infant gut microbiota and metabolome. *bioRxiv*, 698092.
- BADER, G. D. & HOGUE, C. W. 2003. An automated method for finding molecular complexes in large protein interaction networks. *BMC Bioinformatics*, 4, 2.
- BRAY, N. L., PIMENTEL, H., MELSTED, P. & PACHTER, L. 2016. Near-optimal probabilistic RNA-seq quantification. *Nat Biotechnol*, 34, 525-7.
- BULT, C. J., BLAKE, J. A., SMITH, C. L., KADIN, J. A., RICHARDSON, J. E. & MOUSE GENOME DATABASE, G. 2019. Mouse Genome Database (MGD) 2019. *Nucleic Acids Res*, 47, D801-D806.
- CAPORASO, J. G., KUCZYNSKI, J., STOMBAUGH, J., BITTINGER, K., BUSHMAN, F. D., COSTELLO, E. K., FIERER, N., PENA, A. G., GOODRICH, J. K., GORDON, J. I., HUTTLEY, G. A., KELLEY, S. T., KNIGHTS, D., KOENIG, J. E., LEY, R. E., LOZUPONE, C. A., MCDONALD, D., MUEGGE, B. D., PIRRUNG, M., REEDER, J., SEVINSKY, J. R., TURNBAUGH, P. J., WALTERS, W. A., WIDMANN, J., YATSUNENKO, T., ZANEVELD, J. & KNIGHT, R. 2010. QIIME allows analysis of high-throughput community sequencing data. *Nat Methods*, 7, 335-6.
- CHEN, S., ZHOU, Y., CHEN, Y. & GU, J. 2018. fastp: an ultra-fast all-in-one FASTQ preprocessor. *Bioinformatics*, 34, i884-i890.
- CROFT, D., O'KELLY, G., WU, G., HAW, R., GILLESPIE, M., MATTHEWS, L., CAUDY, M., GARAPATI, P., GOPINATH, G., JASSAL, B., JUPE, S., KALATSKAYA, I., MAHAJAN, S., MAY, B., NDEGWA, N., SCHMIDT, E., SHAMOVSKY, V., YUNG, C., BIRNEY, E., HERMJAKOB, H., D'EUSTACHIO, P. & STEIN, L. 2011. Reactome: a database of reactions, pathways and biological processes. *Nucleic Acids Res*, 39, D691-7.
- CUNNINGHAM, F., ACHUTHAN, P., AKANNI, W., ALLEN, J., AMODE, M. R., ARMEAN, I. M., BENNETT, R., BHAI, J., BILLIS, K., BODDU, S., CUMMINS, C., DAVIDSON, C., DODIYA, K. J., GALL, A., GIRON, C. G., GIL, L., GREGO, T., HAGGERTY, L., HASKELL, E., HOURLIER, T., IZUOGU, O. G., JANACEK, S. H., JUETTEMANN, T., KAY, M., LAIRD, M. R., LAVIDAS, I., LIU, Z., LOVELAND, J. E., MARUGAN, J. C., MAUREL, T., MCMAHON, A. C., MOORE, B., MORALES, J., MUDGE, J. M., NUHN, M., OGEH, D., PARKER, A., PARTON, A., PATRICIO, M., ABDUL SALAM, A. I., SCHMITT, B. M., SCHUILENBURG, H., SHEPPARD, D., SPARROW, H., STAPLETON, E., SZUBA, M., TAYLOR, K., THREADGOLD, G., THORMANN, A., VULLO, A., WALTS, B., WINTERBOTTOM, A., ZADISSA, A., CHAKIACHVILI, M., FRANKISH, A., HUNT, S. E., KOSTADIMA, M., LANGRIDGE, N., MARTIN, F. J., MUFFATO, M., PERRY, E., RUFFIER, M., STAINES, D. M., TREVANION, S. J., AKEN, B. L., YATES, A. D., ZERBINO, D. R. & FLICEK, P. 2019. Ensembl 2019. *Nucleic Acids Res*, 47, D745-D751.
- DIXON, P. 2003. VEGAN, a package of R functions for community ecology. *J Veg Sci*, 14, 927-930.
- HUSON, D. H., BEIER, S., FLADE, I., GORSKA, A., EL-HADIDI, M., MITRA, S., RUSCHEWEYH, H. J. & TAPPU, R. 2016. MEGAN Community Edition - Interactive Exploration and Analysis of Large-Scale Microbiome Sequencing Data. *PLoS Comput Biol*, 12, e1004957.
- JALILI, V., AFGAN, E., GU, Q., CLEMENTS, D., BLANKENBERG, D., GOECKS, J., TAYLOR, J. & NEKRUTENKO, A. 2020. The Galaxy platform for accessible, reproducible and collaborative biomedical analyses: 2020 update. *Nucleic Acids Res*.

- KINSELLA, R. J., KAHARI, A., HAIDER, S., ZAMORA, J., PROCTOR, G., SPUDICH, G., ALMEIDA-KING, J., STAINES, D., DERWENT, P., KERHORNOU, A., KERSEY, P. & FLICEK, P. 2011. Ensembl BioMarts: a hub for data retrieval across taxonomic space. *Database (Oxford)*, 2011, bar030.
- KIU, R., BROWN, J., BEDWELL, H., LECLAIRE, C., CAIM, S., PICKARD, D., DOUGAN, G., DIXON, R. A. & HALL, L. J. 2019. Genomic analysis on broiler-associated *Clostridium perfringens* strains and exploratory caecal microbiome investigation reveals key factors linked to poultry necrotic enteritis. *Animal Microbiome*, 1, 12.
- KOPYLOVA, E., NOE, L. & TOUZET, H. 2012. SortMeRNA: fast and accurate filtering of ribosomal RNAs in metatranscriptomic data. *Bioinformatics*, 28, 3211-7.
- MI, H., MURUGANUJAN, A., EBERT, D., HUANG, X. & THOMAS, P. D. 2019a. PANTHER version 14: more genomes, a new PANTHER GO-slim and improvements in enrichment analysis tools. *Nucleic Acids Res*, 47, D419-D426.
- MI, H., MURUGANUJAN, A., HUANG, X., EBERT, D., MILLS, C., GUO, X. & THOMAS, P. D. 2019b. Protocol Update for large-scale genome and gene function analysis with the PANTHER classification system (v.14.0). *Nat Protoc*, 14, 703-721.
- MI, H. & THOMAS, P. 2009. PANTHER pathway: an ontology-based pathway database coupled with data analysis tools. *Methods Mol Biol*, 563, 123-40.
- MUDUNURI, U., CHE, A., YI, M. & STEPHENS, R. M. 2009. bioDBnet: the biological database network. *Bioinformatics*, 25, 555-6.
- PIMENTEL, H., BRAY, N. L., PUENTE, S., MELSTED, P. & PACHTER, L. 2017. Differential analysis of RNA-seq incorporating quantification uncertainty. *Nat Methods*, 14, 687-690.
- QUAST, C., PRUESSE, E., YILMAZ, P., GERKEN, J., SCHWEER, T., YARZA, P., PEPLIES, J. & GLOCKNER, F. O. 2013. The SILVA ribosomal RNA gene database project: improved data processing and web-based tools. *Nucleic Acids Res*, 41, D590-6.
- R DEVELOPMENT CORE TEAM 2010. R: A language and environment for statistical computing. R Foundation for Statistical Computing. Vienna, Austria.
- SEGATA, N., IZARD, J., WALDRON, L., GEVERS, D., MIROPOLSKY, L., GARRETT, W. S. & HUTTENHOWER, C. 2011. Metagenomic biomarker discovery and explanation. *Genome Biol*, 12, R60.
- SHANNON, P., MARKIEL, A., OZIER, O., BALIGA, N. S., WANG, J. T., RAMAGE, D., AMIN, N., SCHWIKOWSKI, B. & IDEKER, T. 2003. Cytoscape: a software environment for integrated models of biomolecular interaction networks. *Genome Res*, 13, 2498-504.
- TANG, Y., HORIKOSHI, M. & LI, W. X. 2016. ggfortify: Unified Interface to Visualize Statistical Result of Popular R Packages. *The R Journal*, 8.
- TUREI, D., KORCSMAROS, T. & SAEZ-RODRIGUEZ, J. 2016. OmniPath: guidelines and gateway for literature-curated signaling pathway resources. *Nat Methods*, 13, 966-967.
- WARNES, G. R., BOLKER, B., BONEBAKKER, L., GENTLEMAN, R., HUBER, W., LIAW, A., LUMLEY, T., MAECHLER, M., MAGNUSSON, A., MOELLER, S., SCHWARTZ, M. & VENABLES, B. 2016. gplots: Various R Programming Tools for Plotting Data. R package version 3.0.1 ed.
- WICKHAM, H. 2016. *ggplot2: Elegant Graphics for Data Analysis*, New York, Springer-Verlag.
- ZERBINO, D. R., ACHUTHAN, P., AKANNI, W., AMODE, M. R., BARRELL, D., BHAI, J., BILLIS, K., CUMMINS, C., GALL, A., GIRON, C. G., GIL, L., GORDON, L., HAGGERTY, L., HASKELL, E., HOURLIER, T., IZUOGU, O. G., JANACEK, S. H., JUETTEMANN, T., TO, J. K., LAIRD, M. R., LAVIDAS, I., LIU, Z., LOVELAND, J. E., MAUREL, T., MCLAREN, W., MOORE, B., MUDGE, J., MURPHY, D. N., NEWMAN, V., NUHN, M., OGEH, D., ONG, C. K., PARKER, A., PATRICIO, M., RIAT, H. S., SCHUILENBURG, H., SHEPPARD, D., SPARROW, H., TAYLOR, K., THORMANN, A., VULLO, A., WALTZ, B., ZADISSA, A., FRANKISH, A., HUNT, S. E., KOSTADIMA, M., LANGRIDGE, N., MARTIN, F. J., MUFFATO, M., PERRY, E., RUFFIER, M., STAINES, D. M., TREVANION, S. J., AKEN, B. L., CUNNINGHAM, F., YATES, A. & FLICEK, P. 2018. Ensembl 2018. *Nucleic Acids Res*, 46, D754-D761.